Kaempferol-phospholipid complex: formulation, and evaluation of improved solubility, *in vivo* bioavailability, and antioxidant potential of kaempferol.

Darshan R. Telang[a], Arun T. Patil[a], Anil M. Pethe[b], Amol A. Tatode[a], Sridhar Anand[c], Vivek S. Dave[c*]

[a] Department of Pharmaceutical Sciences, R.T.M. Nagpur University, Nagpur, Maharashtra, India
[b] SPP School of Pharmacy & Technology Management, Pharmaceutics Division, SVKM's NMIMS University, Mumbai, Maharashtra, India
[c] St. John Fisher College, Wegmans School of Pharmacy, Rochester, NY, USA

Received: November 17, 2016; *Accepted:* November 27, 2016

Original Article

ABSTRACT

The current work describes the formulation and evaluation of a phospholipid complex of kaempferol to enhance the latter's aqueous solubility, *in vitro* dissolution rate, *in vivo* antioxidant and hepatoprotective activities, and oral bioavailability. The kaempferol-phospholipid complex was synthesized using a freeze-drying method with the formulation being optimized using a full factorial design (3^2) approach. The results include the validation of the mathematical model in order to ascertain the role of specific formulation and process variables that contribute favorably to the formulation's development. The final product was characterized and confirmed by Differential Scanning Calorimetry (DSC), Fourier Transform Infrared Spectroscopy (FTIR), Proton Nuclear Magnetic Resonance Spectroscopy (^{1}H-NMR), and Powder X-ray Diffraction (PXRD) analysis. The aqueous solubility and the *in vitro* dissolution rate were enhanced compared to that of pure kaempferol. The *in vivo* antioxidant properties of the kaempferol-phospholipid complex were evaluated by measuring its impact on carbon tetrachloride (CCl_4)-intoxicated rats. The optimized phospholipid complex improved the liver function test parameters to a significant level by restoration of all elevated liver marker enzymes in CCl_4-intoxicated rats. The complex also enhanced the *in vivo* antioxidant potential by increasing levels of GSH (reduced glutathione), SOD (superoxide dismutase), catalase and decreasing lipid peroxidation, compared to that of pure kaempferol. The final optimized phospholipid complex also demonstrated a significant improvement in oral bioavailability demonstrated by improvements to key pharmacokinetic parameters, compared to that of pure kaempferol.

KEY WORDS: Phospholipids, solubility, dissolution, bioavailability, antioxidant

INTRODUCTION

Kaempferol is a bioflavonoid that is commonly present in many fruits and vegetables. It is known to be a potential antioxidant based on its use in plant-derived foods and traditional medicines (1). Following oral administration, kaempferol has been reported to produce a range of pharmacological activities including antioxidant, anti-cancer, anti-inflammatory, hepato-protective, neuroprotective, and osteogenic activities(2-7). This makes

*Corresponding author: Vivek S. Dave, St. John Fisher College, Wegmans School of Pharmacy, Rochester, NY, 14534, Tel: +1-585-385-5297, Fax: +1-585-385-5295, E-mail: vdave@sjfc.edu

kaempferol an attractive formulation target and subject of this investigation.

Despite these positive and favorable health benefits of kaempferol, its low bioavailability and rapid metabolism impair its oral delivery. Following oral administration, kaempferol undergoes extensive first-pass hepatic metabolism through phase II reactions *viz.* methylation, sulfation, or glucuronidation (8). Keeping in mind the potential health benefits listed above, we have sought to develop the appropriate formulation technique to enhance kaempferol's poor absorption and oral bioavailability.

Enhancement of bioavailability is a well-studied phenomenon. Numerous emerging formulation techniques and strategies for the improvement of oral bioavailability have been described in literature. These include liposomes, solid lipid nanoparticles, and self-nanoemulsifying drug delivery systems (SNEDDS). Seguin *et. al.* formulated fisetin-based liposomes to improve its bioavailability and anti-tumor efficacy; the results demonstrated that the liposomal formulation enhanced the relative bioavailability up to 47-fold, as compared to free fisetin (9). Ruan *et. al.* developed a self-nanoemulsifying drug delivery system (SNEDDS) for the delivery of matrine (11). Their results showed that the relative bioavailability in rat serum increased nearly 10-fold compared to free mangiferin. According to these formulation strategies, the poor absorption and oral bioavailability of these phytocompounds were found to progress in excellent manner when complexed with phospholipids. The phospholipids act as a biocompatible carrier system for most of the phytocompounds for improving their poor aqueous solubility, *in vitro* dissolution rate, poor absorption, oral bioavailability, and pharmacological activity. Previously published reports show that the kaempferol exhibits good hepatoprotective and antioxidant effects.

Zhang *et. al.* reported that kaempferol-phospholipids complex in an equimolar ratio (1:1), enhanced the aqueous solubility, *in vitro* dissolution rate, and pharmacokinetic and oral bioavailability in rats (12). However, this study was limited in several aspects including the lack of formulation optimization, the dissolution being carried out for only 2 hours, the lack of reported improvements in bioavailability, and the lack of *in vivo* antioxidant studies. The current work presents a systematic and a comprehensive study on the formulation of kaempferol-phospholipid complex, by including a more elaborate physical and functional characterization. In this study, kaempferol-phospholipids complex was prepared by freeze-drying technique to produce a stable complex in a powder form with spherical particle morphology. A full factorial design (3^2) strategy was employed to understand the influence of various formulation/process variables and to optimize the formulation. A detailed physical characterization of the design-optimized complex was carried out by particle size analysis, zeta potential measurements, thermal analysis, infrared analysis, powder x-ray diffraction analysis, proton nuclear magnetic resonance spectroscopy, and solubility analysis. The prepared complex was further functionally characterized by *in vitro* dissolution studies, *in vivo* antioxidant and hepatoprotective activity, and pharmacokinetic analysis.

MATERIALS AND METHODS

Materials

Kaempferol (~ 99% pure) was obtained from Imam International Group (Pharmaceutical) Co., Ltd., Tianjin, China. Phospholipon® 90H (>90% pure) was received as a gift from Lipoid GmbH, Ludwigshafen, Germany. Carbon tetrachloride, chloroform, 1,4-dioxane, ethylene diamine tetra acetic acid (EDTA), 5,5'-dithiobis (2-nitrobenzoic acid) (DTNB), sodium chloride, and sodium lauryl sulfate (SLS) were obtained from Loba Chemicals Pvt. Ltd.,

Mumbai, India. *n*-hexane, *n*-octanol, *m*-phosphoric acid, thiobarbituric acid (TBA), and trichloroacetic acid (TCA) were obtained from Sigma Chemicals, Sigma-Aldrich Corporation, St. Louis, MO. All other chemicals used in this investigational work were of analytical grade.

Formulation of the kaempferol-phospholipid complex (KPLC)

The kaempferol-phospholipid complex (KPLC) was prepared according to the method reported earlier (13). Briefly, kaempferol (Mol. Wt. 286.24) and Phospholipon® 90H (Mol. Wt. 790) were weighed accurately and placed in a 100 ml round bottom flask. Based on the exploratory experiments carried out earlier, kaempferol and Phospholipon® 90H were used in molar ratios of 1:1, 1:2, and 1:3. Both ingredients were dissolved in 1, 4-dioxane (20 ml) and refluxed. The reflux reactions were carried out at 40°C, 50°C, and 60°C using a water bath for a period of two hours. After two hours, the reaction mixture was freeze-dried using a lyophilizer (Model: MSW-137, Macro Scientific Works Pvt. Ltd., New Delhi, India). The resulting lyophilized KPLC was placed in amber colored glass vials, flushed with nitrogen, and stored at room temperature until further use.

Estimation of kaempferol in the prepared KPLC (% yield)

The extent of kaempferol incorporation in the prepared complex was estimated using a spectrophotometric method described previously (14). Briefly, accurately weighed KPLC (~10 mg kaempferol) was dispersed in 5 ml chloroform. The formed complex and pure Phospholipon® 90H were dissolved in chloroform. Free/non-complexed kaempferol remains insoluble in chloroform and precipitates out. The dispersion was then filtered using a filter paper (Whatman® quantitative filter paper, ash-less, Grade 41, Sigma-Aldrich Corporation, St. Louis, MO). The non-complexed/free kaempferol residue was air-dried, dissolved in methanol, and after appropriate dilutions, analyzed on a UV-visible spectrophotometer (Model: V-630, JASCO International Co. Ltd., Tokyo, Japan) at 365 nm for kaempferol.

Design of Experiments

Preliminary studies carried out in-house and reports published elsewhere identified the main factors and their ranges in influencing the formation of KPLC (15). These factors were drug: phospholipid ratio (X_1, w: w) and the reaction temperature (X_2, ºC), and were chosen at three levels (low, middle, and high) for each factor resulting in a full-factorial design (3^2) composed of nine independent experimental trials. The dependent variable for the study was % yield, i.e. the fraction of kaempferol entrapped by weight in the prepared complex. All nine combinations of selected independent variables were used to carry out the experiments. The results of these experiments were analyzed using a mathematical model described by the Equation 1 below, exhibiting coefficient effects, interactions, and polynomial terms.

$$Y = b_0 + b_1X_1 + b_2X_2 + b_3X_{12} + b_4X_{22} + b_5X_1X_2 \quad \text{Eq. 1}$$

In this equation, Y is the % yield, b is the coefficient of the independent variable X. The independent effects of both factors at different levels are represented as the main effects, X_1 and X_2. The combined effect of the independent variables is shown by the interaction term X_1X_2. The non-linearity of the response is described by the polynomial terms X_{12} and X_{22}. Table 1 shows the experimental design and the actual values of the independent variables. Table 2 shows the experimentally obtained values of the dependent variable, i.e. % yield for each experiment.

Table 1 Coded levels and "real" values for each factor

VARIABLES	LEVELS		
	-1	0	+1
Independent	**Real values**		
Kaempferol : Phospholipids ratio (X_1, w:w)	1:1	1:2	1:3
Reaction temperature (X_2, ºC)	40	50	60
Dependent			
Extent of complexation or Yield (*Y*, % w/w)			

Table 2 Full factorial design (3^2) experimental trial batches, with obtained yield values (%, w/w)

EXPERIMENTAL TRIALS	X_1	X_2	EXTENT OF COMPLEXATION, OR YIELD* (%, w/w)
1	0	+1	88.49 ± 1.48
2	0	0	89.27 ± 0.82
3	-1	-1	92.80 ± 0.75
4	+1	+1	84.15 ± 0.67
5	+1	-1	81.68 ± 1.61
6	-1	0	95.25 ± 1.17
7	+1	0	84.70 ± 1.53
8	0	-1	86.26 ± 0.91
9	-1	+1	93.49 ± 1.32

*Values are represent mean ± Std. Dev. (n = 3)

Physicochemical characterization

Particle size analysis and zeta potential

The particle size distribution of the prepared KPLC was analyzed using Photon Cross-Correlation Spectroscopy (PCCS) with dynamic light scattering setup (16). In a sample vial, ~5 mg of KPLC powder was dispersed in 10 ml deionized water. The analyzer (Model: NANOPHOX, Sympatec GmbH, Clausthal-Zellerfeld, Germany) with a sensitivity range of 1 nm to 10 µm was used to analyze this dispersion. The software associated with the instrument was used to optimize the count rate by appropriate positioning of the dispersion sample vial. The measurements were carried out at 25ºC.

The prepared KPLC was also evaluated for physical stability by analyzing its zeta potential using Nano particle analyzer (Model: NanoPlusTM-2, Particulate systems, Norcross, GA, USA) equipped with dynamic light scattering. The zeta potential of the sample was measured in the sensitivity range of +200 to -200 mV.

Differential Scanning Calometry (DSC)

The thermal behavior of the samples, *viz.*, pure kaempferol, pure Phospholipon® 90H, the physical mixture (PM) of kaempferol and Phospholipon® 90H, and the prepared KPLC was analyzed by differential scanning calorimetry (Model: DSC-1 821e, Mettler-Toledo AG, Analytical, Schwerzenbach, Switzerland). The instrument was calibrated with a high-purity indium standard, and continuously purged with dry nitrogen (50 ml/min) to provide a non-oxidizing environment. Each sample (2.0 ± 0.2 mg) was subjected to a single heating cycle at a heating rate of 10°C min^{-1}, with the temperature ranging from 40°C to 400°C. The instrument software (Universal Analysis 2000) was used to analyze the thermal events associated with the samples.

Fourier Transform Infrared Spectroscopy (FTIR)

A Fourier-transform infrared spectrometer (Model: FTIR-8300, Shimadzu, Kyoto, Japan) was used to study the physicochemical characteristics of pure kaempferol, pure Phospholipon® 90H, the physical mixture of kaempferol and Phospholipon® 90H (PM), and the prepared KPLC. In brief, previously dried samples (~2 mg) were weighed individually and transferred into agate mortar and pestle. The individually weighed samples were mixed uniformly with potassium bromide (KBr, FT-IR grade, ~200 mg) to form a homogenous mixture. This mixture was compressed at a pressure of 10/Nm^2 Ton to obtain thin,

transparent discs on a mini hand press (Model: MHP - 1, P/N - 200-66747-91, Shimadzu, Kyoto, Japan). The sample discs were scanned to obtain infrared spectra in the wavelength range of 4000 to 400 cm^{-1} at a resolution of 4 cm^{-1}. The obtained spectra were processed and analyzed using instrument software (IRsolution FTIR control software, version 1.10).

Proton Nuclear Magnetic Resonance (^{1}H-NMR)

^{1}H-NMR spectroscopy was used to compare the carbon-hydrogen framework of individual components as well as the prepared complex. The individual samples of pure kaempferol, pure Phospholipon® 90H, PM, and KPLC were analyzed to obtain ^{1}H-NMR spectra on a 400 MHz FT-NMR spectrometer (Bruker Advance II, Bruker, Rheinstatten, Germany).

Powder X-ray Diffractometry (PXRD)

The crystal state of pure kaempferol, Phospholipon® 90H, PM, and KPLC was analyzed using a powder x-ray diffractometer (Model: D8 ADVANCE, Bruker AXS, Inc., Madison, WI, USA) accompanied by a Bragg-Brentano geometry (θ/2θ) optical setup. In brief, an accurately weighed (~1 g) sample was mounted into the sample holder. The diffractometer was equipped with a CuKβ anode x-ray monochromatic radiation generating tube source. The sample was irradiated at a wavelength of λ = 1.5406 Å with photon energy in the range of 100 eV to 100 keV. The functional voltage and current were maintained at 30 mV and 10 mA, respectively. A one-dimensional detector (LYNXEYE™) was used to process and convert the individual signal to a spectrum. The spectra of the scanned samples were obtained on the 2θ scale with a diffraction angle range of 3° 2θ to 60° 2θ at a count rate of five seconds.

Solubility analysis

Pure kaempferol, PM, and KPLC were analyzed for their aqueous and n-octanol solubilities using a method previously reported by Saoji, *et. al.* (16). Briefly, an excess amount of each sample was transferred to a sealed glass vial containing 5 ml of water/or n-octanol. This dispersion was allowed to agitate on a water bath shaker (Model: RSB-12, Remi house, Mumbai, India) for 24 hours. The agitated dispersion was centrifuged using a microcentrifuge (Model: RM-12C, Angle Rotor Head, Remi House, Goregaon (E), Mumbai, India) for 25 minutes at 1500 RPM and filtered through a membrane filter (0.45 μ). An aliquot of this filtrate was suitably diluted with water or n-octanol, and assayed using UV-visible spectrophotometer (Model: V-630, JASCO International Co. Ltd., Tokyo, Japan) at 365 nm for kaempferol. All experiments were carried out at room temperature (25°C).

Functional characterization

In vitro dissolution studies

The dissolution behavior of pure kaempferol and the prepared KPLC was analyzed using a dialysis method previously reported by Maiti, *et. al.* (17). Briefly, the dissolution study was carried out using a dialysis bag prepared from a membrane (LA393, Dialysis Membrane-70, HiMedia Laboratories, Mumbai, India) of fixed dimensions (17.5 mm x 28.46 mm) and a capacity of 2.41 ml/min. The membrane was reported to retain molecules over 12000 KDa. The membrane, after pre-treatment according to the manufacturer's instructions, was tied to form the dialysis bag. The samples of pure kaempferol suspension (2 ml, 2 mg/ml of kaempferol) or the prepared KPLC (~4 mg kaempferol) were placed in the bag. The bag was suspended vertically into a beaker containing phosphate-buffered saline (PBS, 200 ml, pH 7.4) and Tween® 20 (1 % v/v) as a surfactant. The entire assembly was stirred at 50

rpm using a magnetic stirrer, and maintained at a temperature of 37.0 ± 2.0°C. 5 ml aliquots of the sample were withdrawn at specific time intervals, and analyzed on a UV-visible spectrophotometer (Model: V-630, JASCO International Co. Ltd., Tokyo, Japan) at 365 nm for kaempferol.

In vivo antioxidant activity

The *in vivo* antioxidant activity of pure kaempferol and the optimized KPLC was comparatively evaluated in a rodent model. This well-established method for the investigation uses carbon tetrachloride (CCl_4) – induced oxidative toxicity in rats, and has been reported earlier in the literature (17, 18). The Institutional Animal Ethics Committee (IAEC) of the University Department of Pharmaceutical Sciences (UDPS), R. T. M. Nagpur University, Nagpur, India approved the experimental protocol for the study (UDPS/IAEC/2013–14/05, dated February 14, 2014). All the investigation procedures followed the ethical guidelines provided by the Committee for the Purpose of Control and Supervision of Experiments on Animals (CPCSEA).

Animals

The animals used for the evaluation of *in vivo* antioxidant activity of pure kaempferol and the optimized KPLC were male and female albino rats (Wistar strain, bred in-house, 150-200 grams). These animals were housed in colony cages at controlled temperature (25 ± 5°C) and humidity (50 ± 5% RH) conditions, with a 12 hour light/dark cycle. The food (pellet chow, Brooke Bond, Lipton, India) and water were provided *ad libitum*.

Dosing and sample collection

The experimental animals were segregated into four groups of six animals each. Group I received the vehicle, i.e. Tween® 20 (1% v/v, p.o.) in distilled water for seven days, and served as blank (negative control). Group II received the single dose of a mixture of CCl_4 and olive oil (1:1, 5ml/kg, i.p.) on the seventh day, and served as positive control. Group III received a pure kaempferol suspension containing 1% v/v of Tween® 20 (25 mg/kg, p.o.) for seven days. Group IV received the KPLC suspension containing 1% v/v of Tween® 20 (~25 mg/kg, p.o.) for seven days. Additionally, on the seventh day, both the groups III and IV also received a single dose of mixture of CCl_4 and olive oil (1:1, 5ml/kg, i.p.).

On the eighth day, following 24 hours of CCl_4 intoxication, all groups of animals were euthanized by cervical decapitation under light ether anesthesia. The blood samples from all the animals were collected into a heparinized tube and centrifuged using a microcentrifuge (Model: RM-12C, Angle Rotor Head, Remi House, Goregaon (E), Mumbai, India). The supernatant plasma samples were employed in the estimation of liver marker enzymes (liver function test). Later, the livers of the animals were removed, and individually washed with ice cold saline solution. These livers were then used to prepare liver homogenate (10% w/v) by homogenizing in 0.1 M phosphate buffer saline (PBS, pH 7.4). The prepared homogenate was then centrifuged using a microcentrifuge (Model: RM-12C, Angle Rotor Head, Remi House, Goregaon (E), Mumbai, India) to obtain a clear supernatant for the estimation of antioxidant marker enzymes.

Liver marker enzyme estimation (liver function test)

Quantitative determination of serum glutamic oxaloacetic transaminase (SGOT), serum glutamic pyruvic transaminase (SGPT), serum alkaline phosphatase (SALP), and total bilirubin was carried out to compare the influence of pure kaempferol and the prepared KPLC on liver function in rats. A well-established method, previously reported by Reitman and

Frankel, was used to estimate SGOT and SGPT levels (19). In brief, the substrates (0.5 ml) for SGOT [α-*L*-alanine (200 mM), or SGPT [*L*-aspartate (200 mM) with 2 mM α-ketoglutarate] were incubated for 5 minutes at 37°C. Rat plasma (0.1 ml) was added to the substrate and phosphate buffer (pH 7.4, 0.1 M) was used to make up the final volume to 1 ml. The mixture was then incubated for 30 minutes (for SGPT) or 60 minutes (for SGOT) at 37°C. 2, 4 – dinitrophenyl hydrazine (0.5 ml, 1 mM) was added as an indicator and the mixture incubated further for 30 minutes. After 30 minutes, sodium hydroxide (5 ml, 0.4 N) was added to the reaction mixture, and the solution was spectroscopically analyzed at 505 nm.

The plasma SALP levels were estimated using '*Grifols-Lucas method*' reported earlier by Kind *et. al.* (20). Briefly, phenyl phosphate substrate (1 ml, 0.5 N) was added to bicarbonate buffer (1 ml, pH 10) and incubated for three minutes at 37°C. Rat plasma (0.1 ml) was added to this solution and the mixture was further incubated for 15 minutes. Following incubation, sodium hydroxide (0.8 ml, 0.5 N), sodium bicarbonate (1.2 ml, 0.5 N), amino-antipyrine (1 ml, 0.6%), and potassium ferricyanide (1 ml, 0.24%) were added to the reaction mixture and thoroughly mixed on a vortex mixer. The solution was then analyzed spectroscopically at 520 nm.

The bilirubin content in rat plasma was estimated using the procedure described by Malloy *et. al.* (21). Briefly, rat plasma (0.25 ml) and sodium nitrate (0.1 ml, 144 mmol/L) were added to an aqueous solution of sulfanilic acid (5 ml, 4 mmol/mL) and incubated for 10 minutes at 37°C. The absorbance of this solution was measured at 670 nm.

Estimation of antioxidant marker enzymes

The quantitative determination of the enzymes *viz.*, glutathione (GSH), superoxide dismutase (SOD), lipid peroxidase (LPO), and catalase (CAT) in rat liver homogenate was carried out to estimate the *in vivo* antioxidant activity of pure kaempferol as well as the prepared KPLC.

A method established earlier by Ellman *et. al.* was used to quantitatively estimate the GSH levels (22). In brief, liver supernatant (0.2 ml), distilled water (1.8 ml), and a precipitating mixture, i.e. *m*-phosphoric acid (1.67 g), EDTA (0.2 g), and NaCl (30 g) in 100 ml distilled water were added to a test tube, vortexed, and centrifuged using a microcentrifuge (Model: RM-12C, Angle Rotor Head, Remi House, Goregaon (E), Mumbai, India). To the separated supernatant (1 ml), phosphate buffer (1.5 ml, 0.1 M), and 5, 5'-dithiobis-(2-nitrobenzoic acid) (DTNB, Ellman's reagent, 0.5 ml) were added and mixed well. The resulting mixture was analyzed at 412 nm on a UV-visible spectrophotometer (Model: V-630, JASCO International Co. Ltd., Tokyo, Japan). The results were expressed as μg/mg of protein.

The SOD was quantified using a method reported by Marklund *et. al.* (23). Briefly, liver supernatant (20 μl), Tris-HCl buffer (2 ml, 75 mM, pH 8.2), EDTA (0.6 ml, 6 mM), and pyrogallol solution (0.5 ml, 30 mM, freshly prepared) were added to a test tube and mixed well. This reaction mixture was spectrophotometrically analyzed at 420 nm at an interval 30 sec for 3 minutes to record any changes in the absorbance over time. A 50% inhibition in the rate of auto-oxidation of pyrogallol was considered to be equivalent to one unit of enzyme activity, and expressed as units/mg of protein.

LPO was quantitatively estimated using a method previously reported by Stocks *et. al.* (24). Briefly, liver supernatant (0.5 ml), sodium lauryl sulfate (0.8%, 0.2 ml), trichloroacetic acid (20%, 1 ml), and thiobarbituric acid (0.8%, 1.5 ml) were added to a test tube and heated for 1 hour at 100°C. The reaction mixture was cooled to room temperature (25°C). After

cooling, distilled water (1 ml) was added to this mixture, and the mixture centrifuged using a microcentrifuge (Model: RM-12C, Angle Rotor Head, Remi House, Goregaon (E), Mumbai, India) to separate the aqueous and the organic layer. The organic layer was collected and analyzed spectroscopically (Model: V-630, JASCO International Co. Ltd., Tokyo, Japan) at 532 nm. The lipid peroxidation was calculated on the basis of the molar extinction coefficient of malondialdehyde (MDA) (1.56 x 105 M^{-1} cm^{-1}), and represented as MDA (nM/g) in hemoglobin.

A method reported previously by Beer *et. al.* was used for the quantitative estimation of CAT (25). Briefly, a reaction mixture was prepared by mixing liver supernatant (0.1 ml), phosphate buffer (1.9 ml, 50 mM, pH 7.4), and freshly prepared hydrogen peroxide (1.0 ml). The reaction mixture was spectroscopically (Model: V-630, JASCO International Co. Ltd., Tokyo, Japan) at 240 nm. The extent of hydrogen peroxide decomposition was correlated to the amount of CAT.

Histopathological studies

On the completion of oral dosing of all the samples, i.e. on the eighth day, all animals were euthanized by cervical decapitation technique. The livers were isolated, washed (in ice cold saline solution), and preserved in neutral buffered formalin (10% v/v) until further processing. The livers were sectioned to the desired size and stained using the hematoxylin-eosin reagent. The stained images were examined using an optical microscope (Model: DM2500, Leica Microsystems Inc., Buffalo Grove, IL), and the images were captured at a magnification of 400× with a digital camera attached.

Oral bioavailability studies

Extraction of kaempferol from plasma and sample preparation

The oral bioavailability after administration of pure kaempferol, or the prepared KPLC was investigated by extracting kaempferol from rat plasma. The extraction procedure was adopted from a previously reported method by Chen *et. al.* (26). Briefly, two groups of six animals each were fasted overnight with access to water *ad libitum*. The first group received a single dose of kaempferol (100 mg/kg, p.o.) and the second group received a single dose of KPLC (~100 mg/kg, p.o. kaempferol). At predetermined time intervals, the animals were anesthetized and blood samples were obtained from the retro-orbital plexus. These samples were collected into Eppendorf® Safe-Lock microcentrifuge tubes (1.5 ml) and centrifuged using a microcentrifuge (Model: RM-12C, Angle Rotor Head, Remi House, Goregaon (E), Mumbai, India) at 3000 rpm for 10 minutes. The separated plasma was collected and stored at -20°C until further use.

Kaempferol was extracted from the collected plasma samples using a liquid-liquid extraction technique. Briefly, a reaction mixture was prepared by adding hydrochloric acid (25%, 200 µl) to the plasma sample (200 µl) in a test tube followed by vortexing the mixture for 3 minutes. The sample was allowed to hydrolyze for 60 minutes on a water bath at 80°C. After allowing to cool to room temperature, ethyl acetate (1 ml) was added, and the mixture vortexed for additional 3 minutes. The mixture was then centrifuged using a microcentrifuge (Model: RM-12C, Angle Rotor Head, Remi House, Goregaon (E), Mumbai, India) at 3000 RPM for 3 minutes to separate the aqueous and the organic layer (I). The aqueous layer was separated and further spiked with ethyl acetate (1 ml), vortexed, and centrifuged at 3000 rpm for 10 minutes to separate the aqueous and the organic layers (II). The organic layers (I and II)

were mixed together, transferred to a centrifuge tube, and dried under a stream of nitrogen. The dried residue was reconstituted in methanol (100 µl) and centrifuged at 15000 RPM for 10 minutes. An aliquot (20 µl) from this solution was analyzed using HPLC (Model: Thermo Scientific™, PDA, USA).

High Performance Liquid Chomatograpy (HPLC) analysis

The quantitative determination of kaempferol in plasma samples was carried out using the HPLC-based analysis described by Chen *et. al.* (26). An automated HPLC system (Thermo Scientific™ UltiMate™ 3000, Thermo Scientific, San Jose, CA, USA) along with a Photo Diode Array (PDA) detector (Thermo Scientific, San Jose, CA, USA) was used to analyze the samples. Hypersil GOLD™ C18 Selectivity LC Column (100mm × 4.6mm), with a particle size of 5 µm, was used as a stationary phase. The mobile phase was composed of a mixture of acetonitrile and phosphoric acid (0.4%), and used for gradient elution. The flow rate of the mobile phase was controlled at 1.0 ml/min to ensure an effective resolution. The column temperature was maintained at 30°C, and the analyte detection wavelength was set at 360 nm. Quercetin was used as an internal standard. The mobile phase composition was optimized to obtain the best possible resolution of kaempferol peaks in the chromatogram. The obtained peaks were analyzed, integrated, and interpreted using the accompanying software.

Pharmacocinetic studies

The concentration-time curve provided the main pharmacokinetic parameters, *i.e.* maximum plasma concentration (C_{max}) and the time to reach maximum concentration (T_{max}). A popular statistical software (WinNonlin®, Version 4.1, Certara USA Inc., Princeton, NJ, USA) was used to calculate other parameters such as half-life ($t_{½}$), area under the plasma concentration-time curve from zero to the time of the final measured sample ($AUC_{0\to t}$), area under the plasma concentration-time curve from zero to infinity ($AUC_{0\to\infty}$), clearance (Cl/F) and volume of distribution (V_z/F), and the relative bioavailability (F).

Statistical analysis

The solubility and other *in vitro* study results are reported as mean ± standard deviation. The results from the liver function test, *in vivo* antioxidant activity, and the pharmacokinetic analysis are reported as mean ± standard error of mean. The statistically significant differences between the sample groups, if any, were analyzed by one-way Analysis of Variance (ANOVA) followed by Dunnett's or Student's *t*-test. The p values of 0.05 or lower were assumed as statistically significant.

RESULTS AND DISCUSSION

Formulation of kaempferol-phosphoolipids complex (KPLC)

The freeze-drying method was used to prepare a stable complex of kaempferol with phospholipids in the current study. Flavonoids are known to be lipophilic molecules that demonstrate fair solubility in organic solvents (27). Bhattacharyya *et. al.* reported the use of dichloromethane (DCM) as a solvent of choice in the preparation of flavonoid-phospholipid complexes (28). Other studies have also reported the use of dichloromethane and/or tetrahydrofuran (THF) as a solvent in the preparation of similar complexes (14, 17, 18, 29). The preliminary solubility studies showed that kaempferol was poorly soluble in the above solvents, leading to the precipitation of kaempferol in DCM and THF. Other organic solvents were explored with respect to kaempferol solubility and the preparation of complex. It was found that the binary solvent combination of 1, 4-dioxane (an aprotic solvent with low dielectric constant) with methanol (a similar aprotic solvent) in a ratio of 7:3 was an

optimal system for the preparation of KPLC.

Full factorial design

Table 2 shows the results obtained from the experimental trials carried out using a 3^2 full factorial design for the extent of KPLC formation. Both the variables studied, i.e. kaempferol:phospholipid ratio (X_1, w:w) and the reaction temperature (X_2, °C), appeared to influence the extent of complexation. The yield (% kaempferol incorporated) values studied ranged between 82 and 95% for the variables studied. A quadratic model relating the yield to the investigated variables was constructed. Conclusions based on the magnitude of the coefficient, as well as, the sign (+, or –) associated with it were drawn using the polynomial equation (Equation 1) resulting from the analysis of data.

$$Y = 89.28 + 5.16X_1 + 0.90X_2 + 0.66X_{12} + 1.91X_{22} + 0.44X_1X_2 \quad \text{Eq. 1}$$

Statistically significant ($p<0.05$) values were observed for the coefficients b_0, b_1, b_2, b_3, b_4, *and* b_5. For this equation, the obtained correlation coefficient ($R^2 = 0.9990$) was found to be in agreement with the predicted coefficient ($R^2 = 0.9884$). Additionally, the estimated F value (629.62) for the model were also found to be significant ($p<0.05$). Finally, the positive sign associated with coefficients (b_1 and b_2) indicated a direct correlation between the studied variables and the yield (%). These observations supported the reliability of the developed model for the study. Figure 1 shows the response surface and contour plot reflecting the influence of the studied variables on the yield (%). The optimal values of the studied variables, i.e. kaempferol: phospholipid ratio (X_1, w:w) and the reaction temperature (X_2, °C) were found to be 1:1, and 50°C for the optimization of KPLC, respectively.

Validation of optimized model

The design-generated optimized variables were used to prepare an independent batch of KPLC formulation with a goal to validate the developed model. The predicted (theoretical) yield from the developed model was compared with the actual yield achieved from the prepared formulation. This comparison revealed that the actual yield (95.1%) was slightly lower, albeit comparable to the model-predicted yield (96.2%). The bias (-1.15%) calculated using Equation 2 below, was also found to be lower than 3%. These results support the validity and robustness of the developed model (30).

$$Bias\,(\%) = \frac{predicted value - observed value}{predicted\ value} x\,100 \quad \text{Eq. 2}$$

Physicochemical characterization

Particle size analysis and zeta potential

The particle size and zeta potential are important physical characteristics of particulate formulations such as KPLC. These parameters are potentially indicative of the physical stability and bioavailability of the formulation in dispersion or suspension form. Nanoparticulate systems, with lower average particle size, are known to exhibit enhanced oral bioavailability. Figure 2(A) shows the particle size distribution of the optimized KPLC formulation. The mean particle size of the prepared KPLC was found to be 141.88 ± 1.23 nm. The polydispersity index (PDI) of the formulation was found to be 0.33 ± 0.012. These findings are in agreement with those reported previously for similar formulations (13, 31).

Zeta potential (ζ), a measure of the surface charge on the particles, is indicative of the physical stability of the formulation in a colloidal dispersion. Previously published

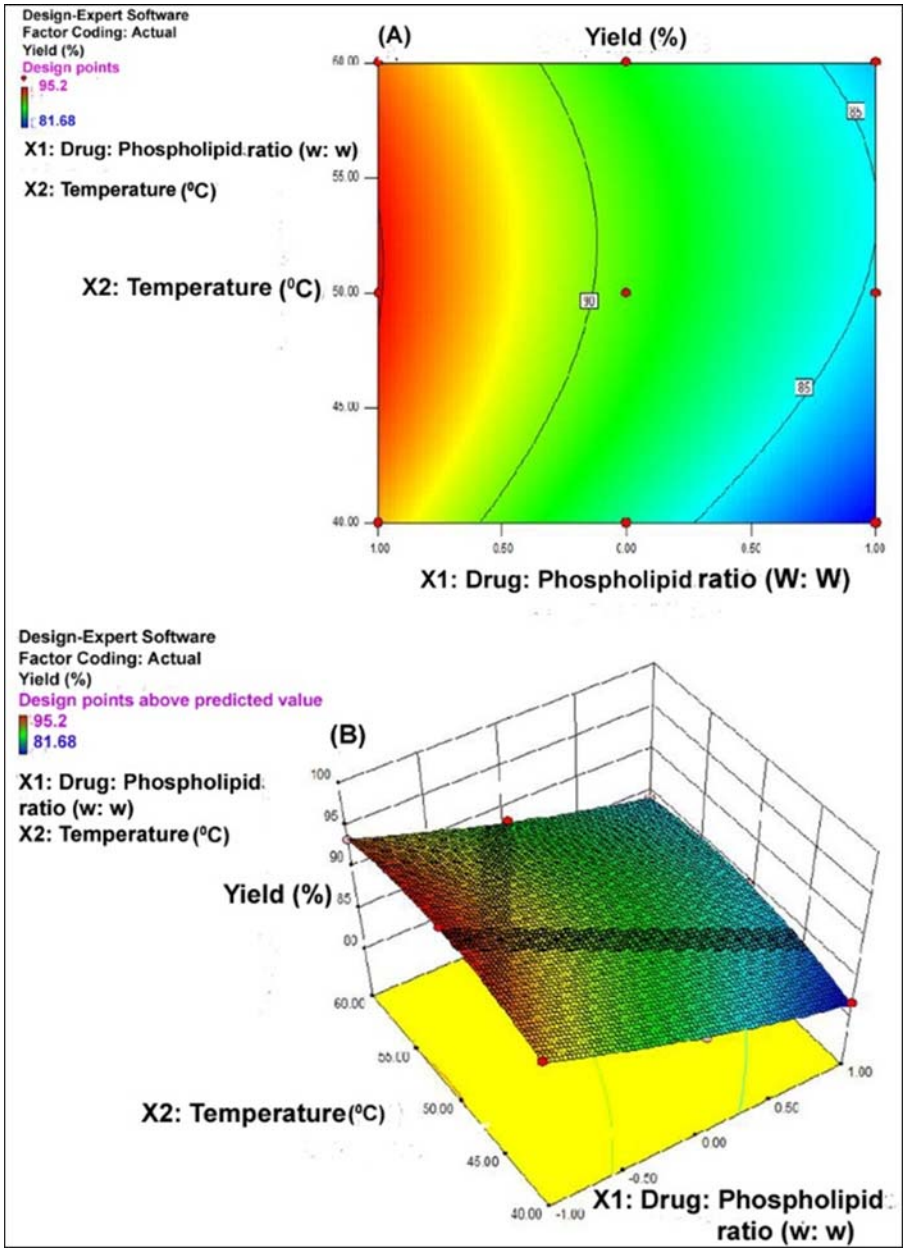

Figure 1 The response surface plot and contour plots of entrapment efficiency (Y, %) as a function of the ratio of kaempferol and Phospholipon® 90H (X_1, w:w), and the reaction temperature (X_2, °C).

reports have suggested that the zeta potential lower than 30 mV is related to particle attraction followed by flocculation, exceeding repulsion forces (14, 32, 33). Figure 2(B) shows the distribution of zeta potential for the prepared KPLC formulation. The zeta potential for the prepared formulation was found to be -18.70 ± 0.20. The zeta potential value depends on the type and composition of phospholipids. In KPLC, the low zeta potential value can be attributed to the involvement of a portion of phospholipids with generation of negative charge in aqueous environment with relatively neutral pH (34). Hence, smaller particle size,

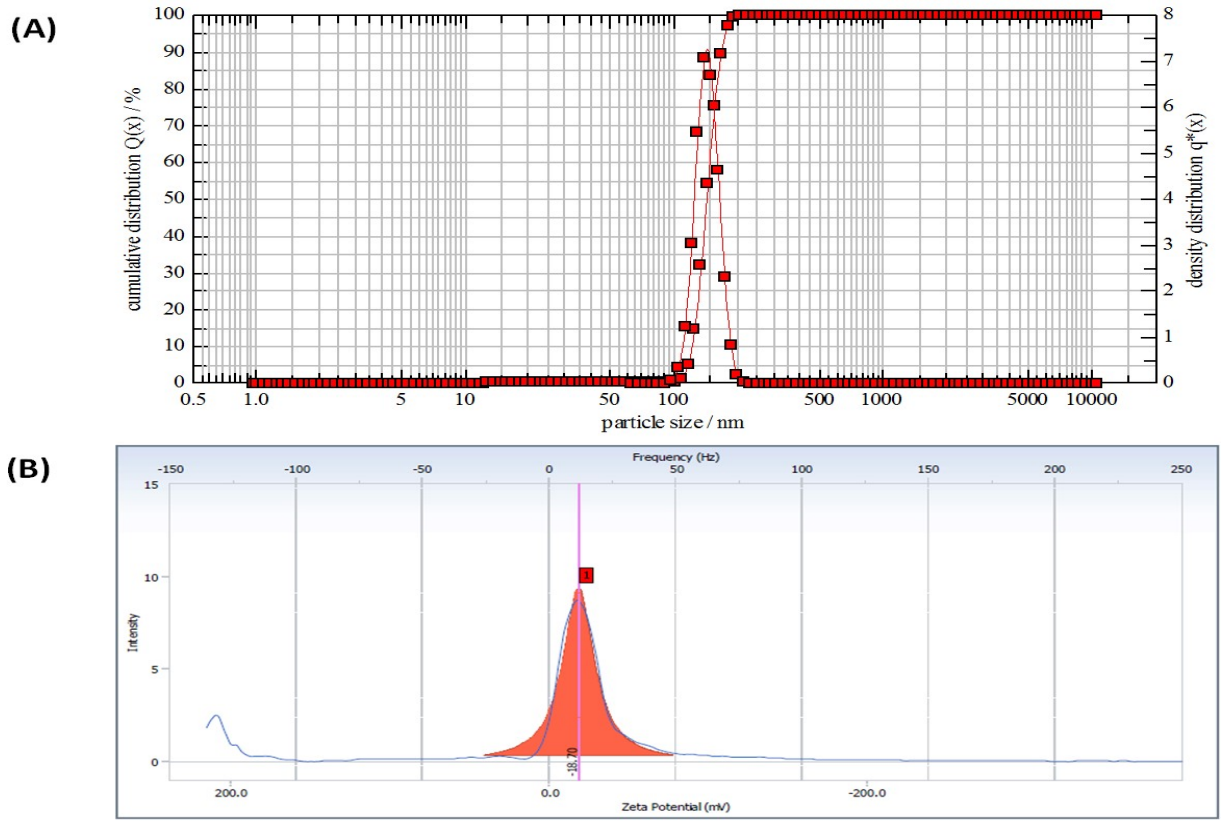

Figure 2 Particle size distribution (A) and zeta potential (B) of the optimized KPLC formulation.

lower polydispersity index and modest zeta potential value for KPLC indicated an acceptable physical stability and suitability for oral administration.

Differential Scanning Calometry (DSC)

For pharmaceutically relevant materials, critical information regarding their physical behaviors such as melting, degradation, physical stability, and compatibility of the formulation components can be reliably obtained by subjecting the samples to controlled temperature changes. Differential scanning calorimetry is among the well-established techniques used for the thermal analysis of such materials. Enthalpy changes, appearance/ disappearance of peaks, and changes to a peak(s) onset time, shape, relative area, as a function of temperature are exhibited in DSC thermograms. Information regarding drug-excipient interactions and formation of new entities is often obtained from DSC analysis of a formulation.

Figure 3 shows the DSC thermogram obtained from the analysis of pure kaempferol (A), pure Phospholipon® 90H (B), PM (C), and KPLC (D). As shown in Figure 3, pure kaempferol (A) exhibited a sharp, endothermic, melting peak at ~285°C. The thermogram also showed a small, broad peak at ~147°C. This peak can be attributed to the loss of water molecules with progressive increase in the temperature (35). The thermogram of pure Phospholipon® 90H (B) in Figure 3 showed two broad endothermic peaks. The first, relatively larger peak at ~67°C, and the second smaller peak at ~85°C. The formation of first peak can be attributed to the melting of the phospholipid molecule. The second peak indicates a controlled phase

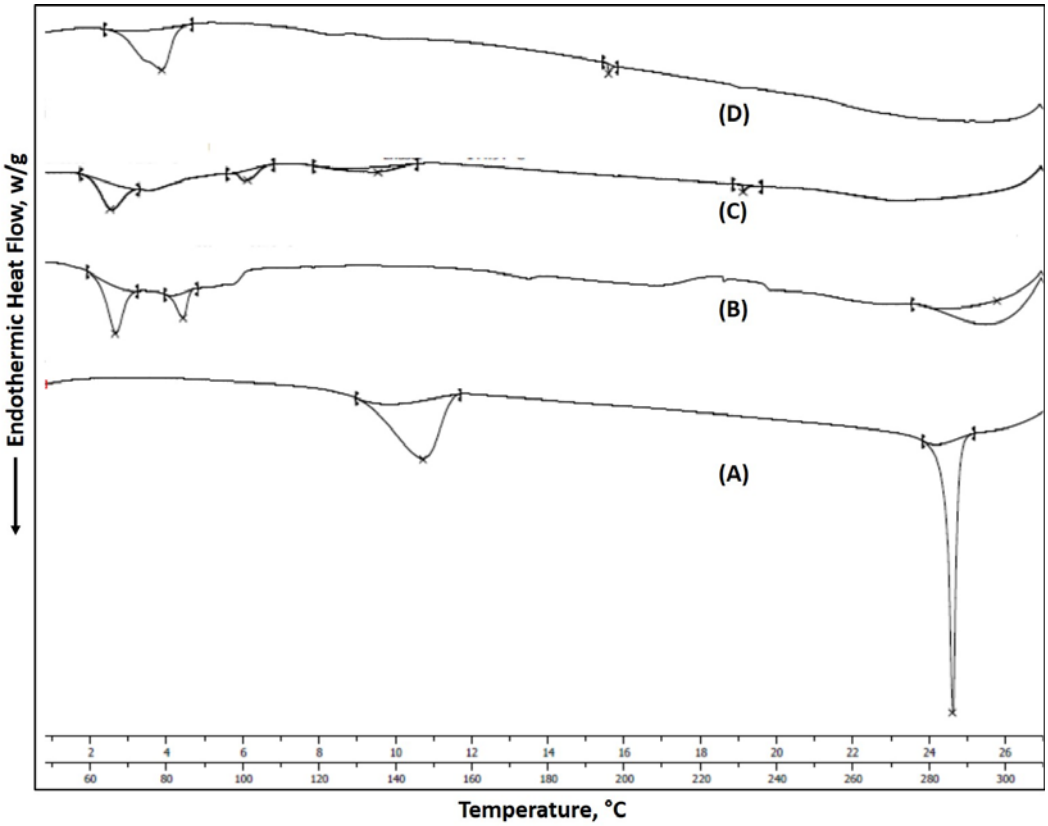

Figure 3 DSC thermograms of (A) pure kaempferol, (B) Phospholipon® 90H, (C) the physical mixture (1:1) of kaempferol and Phospholipon® 90H, and (D) KPLC.

transition, involving conversion from a gel-like structure to a liquid crystalline structure; this occurs through crystalline or isomeric changes along the length of carbon chain of the phospholipid molecule (35-37). The thermogram of the physical mixture (PM) (Figureure 3C) also shows two dissimilar peaks, a smaller endothermic peak at ~67ºC, and a broader peak at ~103ºC. With formulation components like the ones tested in this study, controlled increase in temperature has been reported to cause individual components to form a partial complex *in situ*, which may melt at temperatures lower than the individual components (10). Finally, Figure 3D shows the thermogram of the prepared KPLC. This thermogram displayed a unique and a new endothermic peak at ~80ºC, with the original peaks of kaempferol or Phospholipon® 90H being absent. These results are in agreement with those reported earlier (38). These observations, and the reports published elsewhere, supports the formation of a stable complex of kaempferol (KPLC). Weak intermolecular forces such as hydrogen bonding and van der Waals interactions between the drug and the phospholipid molecule are thought to be contributing to the formation of such complexes (37, 39, 40). The larger phospholipid molecule, with these interactions, likely disperses kaempferol at a molecular level by entrapping kaempferol molecule.

Fourier Transform Infrared Spectroscopy (FTIR)

Figure 4 (A, B, C, and D) shows the FTIR spectra of pure kaempferol, pure Phospholipon® 90H, PM, and the optimized

KPLC formulation. As shown in Figure 4A, the spectra of pure kaempferol displayed characteristic absorption peaks at ~3427 cm^{-1} and ~3317 cm^{-1} (phenolic O-H stretching), ~2954 cm^{-1} and ~2850 cm^{-1} (C-H stretching), and at ~1613 cm^{-1} (C=O stretching). These

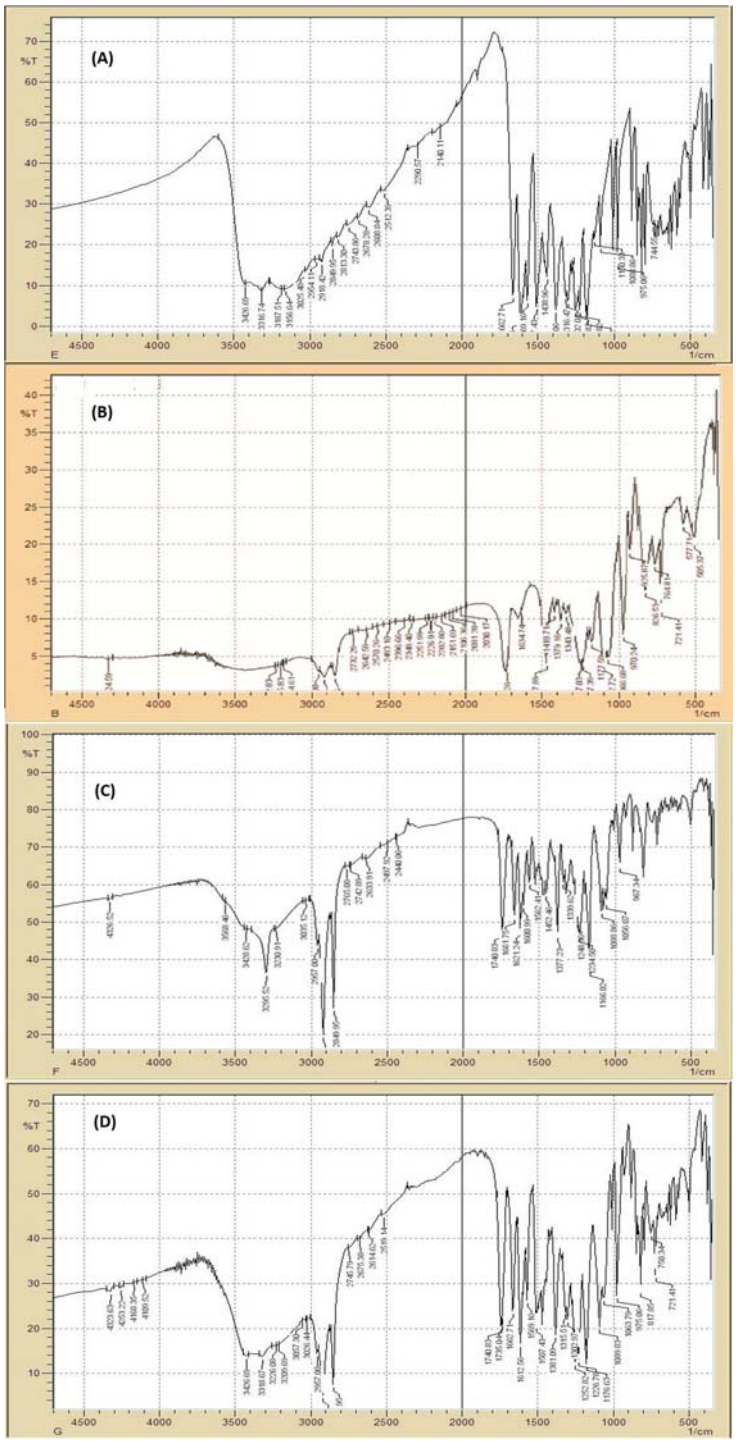

Figure 4 FTIR spectra of (A) pure kaempferol, (B) Phospholipon® 90H, (C) the physical mixture (1:1) of kaempferol and Phospholipon® 90H, and (D) KPLC.

observations are consistent with those reported earlier for kaempferol (41). Figure 4B shows the FTIR spectrum of pure Phospholipon® 90H. The spectrum exhibited the characteristic peaks at ~2918 cm^{-1} and ~2850 cm^{-1} (C-H stretching in the fatty acid chain). Additional signals observed were at ~1738 cm^{-1} (C=O stretching in the fatty acid ester), ~1237 cm^{-1} (P=O stretching), ~1092 cm^{-1} (P–O–C stretching), and at ~970 cm^{-1} [$-N^+ (CH_2)_3$]. Similar results for phospholipid molecules have been reported earlier (42-44). Figure 4C shows the spectrum of the physical mixture (PM), and reveals characteristic signals of the individual components, i.e., kaempferol and Phospholipon® 90H. The peaks were observed at ~3304 cm^{-1}, ~2918 cm^{-1}, ~2850 cm^{-1}, and ~1268 cm^{-1} (36). The FTIR spectrum of KPLC is shown in Figure 4D, and exhibited peaks at ~3319 cm^{-1}, ~2957 cm^{-1}, ~2850 cm^{-1}, ~2918 cm^{-1}, ~1090 cm^{-1}, and ~975 cm^{-1}. When the KPLC spectrum is compared with those of the individual components, i.e. kaempferol, or Phospholipon® 90H, it appeared that the interaction of kaempferol with phospholipids resulted in appearance of novel peaks, disappearance of peaks specific to individual components, as well as shifting of some peaks. The kaempferol specific peaks at ~3317 cm^{-1} and ~2954 cm^{-1} were observed to be shifted to ~3319 cm^{-1} and ~2957 cm^{-1}, respectively. Peaks specific to Phospholipon® 90H were also found to be significantly altered in the KPLC spectrum. These observations support the formation of KPLC as a result of weak intermolecular interactions between kaempferol and phospholipid molecules.

Proton Nuclear Magnetic Resonance (^{1}H-NMR)

The ^{1}H-NMR signal of pure kaempferol and KPLC were recorded at 400 MHz frequency on (δ) scale, and the spectra are shown in Figure 5 (A and B). The ^{1}H-NMR spectrum signal of pure kaempferol (Figure 5A) displayed characteristic chemical shift values (δ, ppm; d_6-DMSO) below: 12.44 (s, 1H), 10.66 (s, 1H,), 10.04 (s, 1H) , 9.24, 8.04 (d, J = 12.0 Hz, 2H), 6.92 (dt, J = 8.8 Hz, 2.4 Hz, 2H), 6.40–6.17 (dd, J = 8.8 Hz, 4 Hz, , 2H), 6.30 (d, J = 2.1 Hz, 1H), 6.09 (d, J = 2.1 Hz, 1H), The chemical shift values (δ) obtained with these signals showed good agreement with the previously published literature (36, 41, 42, 45). The ^{1}H-NMR spectrum signal of Phospholipon® 90H showed chemical shift values (δ, ppm) at 4.85 (1H, s), 4.08–3.96 (br s, 1H), 3.83–3.62 (s, 2H), 3.38 (s, 1H), 3.07 (s, 15H), 2.95 (d, J = 6.8 Hz, 8H), 2.27 (s, 1H), 1.26 (s, 2H, s), 0.95 (s, 23H), 0.57 (s, 3H, s) (41). The ^{1}H-NMR of KPLC (Figure 5B) displayed the following chemical shift values (δ, ppm; d_6-DMSO): 12.42 (s, 1H), 10.75 (s, 1H), 10.04 (s, 1H), 9.19 (s, 1H), 8.21, 8.05 (d, J = 9.0 Hz, 2H), 6.90 (d, J = 9.0 Hz, 2H), 6.39 (d, J = 2.1 Hz, 1H), 6.13 (d, J = 2.1 Hz, 1H), 3.18 (s, 2H), 1.24 (s, 6H). The shifts observed at 1.24 ppm and 3.18 ppm in KPLC, compared to free kaempferol and Phospholipon® 90H relate to the alkyl side chain and N-methyl group. By comparing the chemical shifts among the three compounds, it is clearly evident that weak intermolecular bonding interactions exist between kaempferol and Phospholipon® 90H, which renders the formation of a stable KPLC.

Powder X-Ray Diffractometry (PXRD)

The Figure 6 (A, B, C, and D) shows the diffractograms obtained from the powder x-ray analysis of pure kaempferol, Phospholipon® 90H, PM, and KPLC, respectively. Multiple sharp and intense peaks were observed in the diffractogram of pure kaempferol at 2θ = 9°, 10°, 15°, 26°, and 27° (Figure 6A), in line with its crystalline nature (12, 46). The diffractogram of pure Phospholipon® 90H (Figure 6B) displayed a single, relatively broad peak around 2θ = 21°. The amorphous nature of phospholipid molecule was evident by the absence of any sharp crystalline peak. These observations are in agreement with those reported earlier (47, 48). Figure 6C displays the x-ray diffractogram of a physical mixture of kaempferol and Phospholipon® 90H. The diffraction pattern of the physical mixture

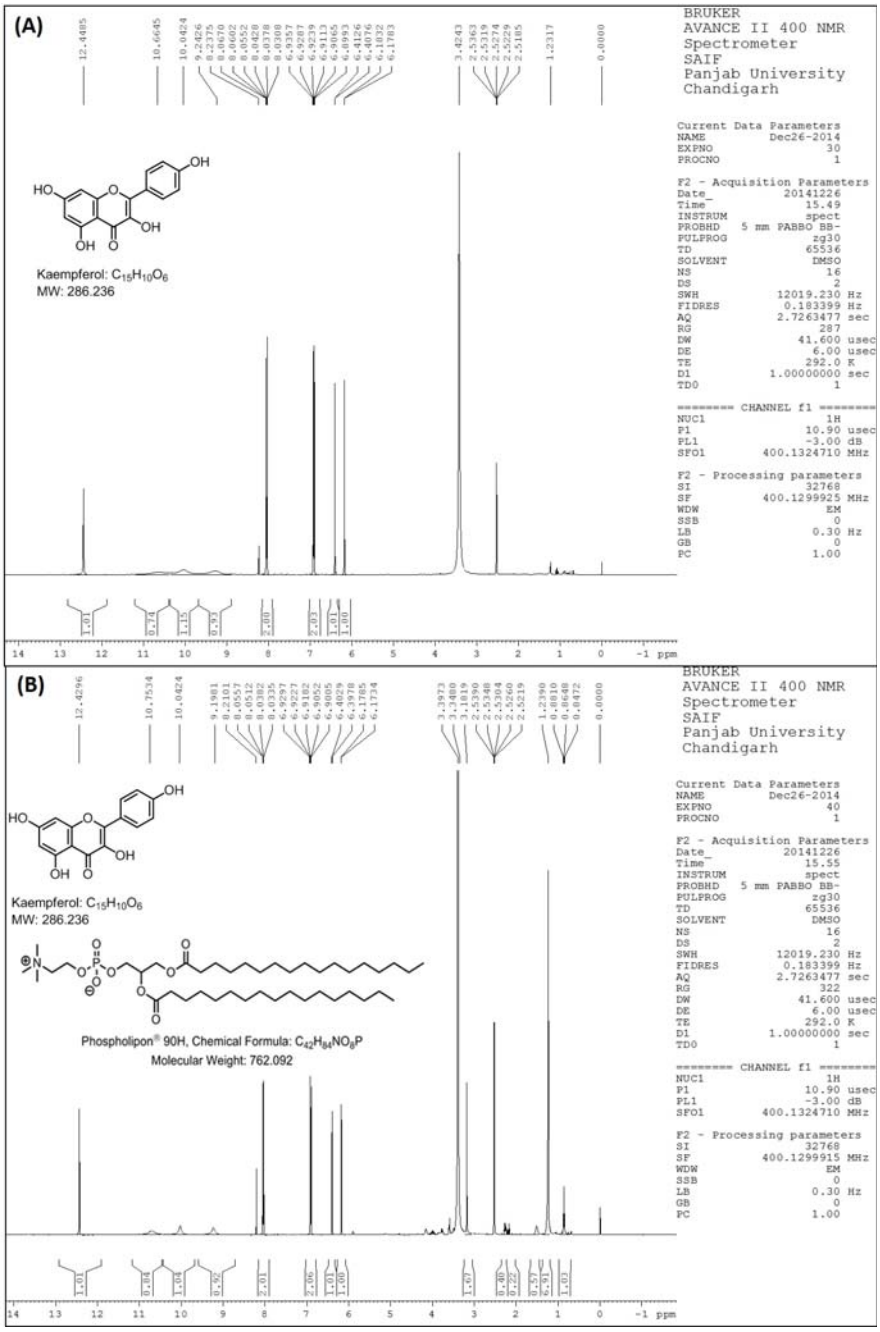

Figure 5 ^{1}H-NMR spectra of (A) kaempferol, and (B) KPLC.

exhibited a few low-intensity crystalline peaks and a relatively broader peak likely associated with kaempferol and Phospholipon® 90H, respectively. Lower amount of kaempferol compared to phospholipid in the mixture, interference by the phospholipid molecule, or *in situ* partial formation of a complex between kaempferol and phospholipids could have possibly caused the observed decrease in the intensity of crystalline peaks. Partial amorphization of kaempferol due to its close association with phospholipid also cannot be ruled out. Finally, as shown in Figure 6D, the diffractogram of KPLC revealed two, broad, ill-

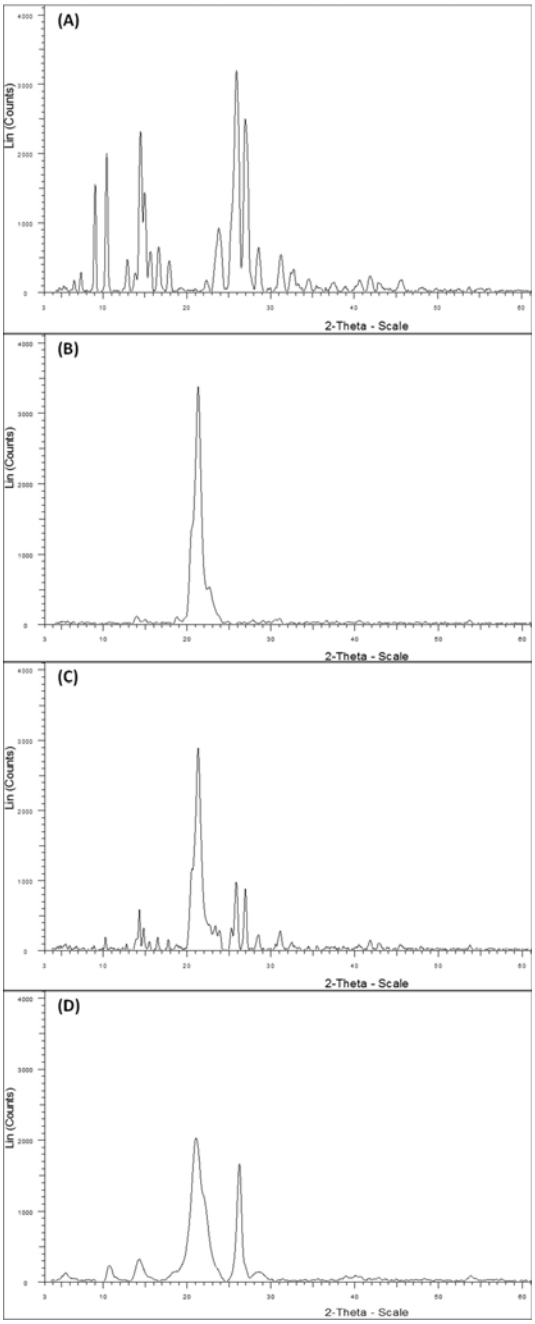

Figure 6 The x-ray diffractograms of (A) pure kaempferol, (B) Phospholipon® 90H, (C) the physical mixture (1:1) of kaempferol and Phospholipon® 90H, and (D) KPLC.

defined, and closely situated peaks at 2θ = 20° and 2θ = 26°. The peak at 2θ = 20° could be associated with the Phospholipon® 90H, whereas the peak observed at 2θ = 26° could be thought of as a remnant signature of kaempferol. Other peaks defining the crystals

of kaempferol were absent. These observations indicate that kaempferol may be molecularly dispersed in a matrix of phospholipid, and a major fraction is present in an amorphized form (49).

Solubility analysis

Table 3 shows the results from solubility analysis of pure kaempferol, PM, and KPLC as measured in water and n-octanol. The aqueous solubility of pure kaempferol was found to be ~1.25 μg/ml; whereas, its solubility in n-octanol was observed to be ~902.73 μg/ml. These observations indicated that kaempferol molecule is predominantly lipophilic in nature and belongs to Class II (low solubility/high permeability) of the Biopharmaceutics Classification System (BCS). The analysis of the physical mixture (PM) revealed that kaempferol solubility in n-octanol remained practically unchanged (~904.68 μg/ml), while its aqueous solubility was found to increase significantly (p<0.01) compared to pure kaempferol. Over 6-fold increase (~8.23 μg/ml) in the aqueous solubility of kaempferol was observed in the physical mixture. This observed increase in kaempferol aqueous solubility can be attributed to the presence of amphiphilic phospholipid molecules in close proximity to kaempferol molecules. The aqueous solubility of kaempferol in the prepared KPLC exhibited a dramatic and significant (p<0.001) increase (~35.68 μg/ml), compared to either pure kaempferol or PM. Over 28-fold increase in aqueous solubility of kaempferol was observed with KPLC compared to that of pure kaempferol. A modest increase (~908.98 μg/ml) in the solubility of kaempferol in n-octanol was also observed with KPLC. The dispersion of kaempferol molecules within the amphiphilic phospholipid molecules, resulting in partial amorphization of kaempferol may be attributed to this observed increase in aqueous solubility of kaempferol in the prepared KPLC (36, 37).

Functional characterization

In vitro dissolution studies

The results of the comparison of dissolution profiles of pure kaempferol with that of the prepared KPLC in phosphate buffer (pH 7.4) are shown in Figure 7. These results show that for the first 5 hours the release profiles of kaempferol and KPLC almost overlapped and there was no significant difference between the profiles. The dissolution of pure kaempferol appeared to reach a plateau, and exhibited maximum dissolution of ~31% at the end of 12 hours. The release of kaempferol from KPLC, however, continued to steadily increase reaching over 70% by the end of 12 hours.

Table 3 Solubility analysis of pure kaempferol, the physical mixture (1:1) of kaempferol and Phospholipon® 90H (PM), kaempferol-Phospholipon® 90H complex (KPLC).

SAMPLE	AQUEOUS SOLUBILITY (μg/ml)*	n-OCTANOL SOLUBILITY (μg/ml)*
Kaempferol	1.25 ± 0.33	902.73 ± 0.29
PM	8.23 ± 0.78	904.68 ± 0.60
KPLC	35.68 ± 1.15	918.98 ± 1.08

*Data expressed as mean ± Std. Dev. (n = 3)

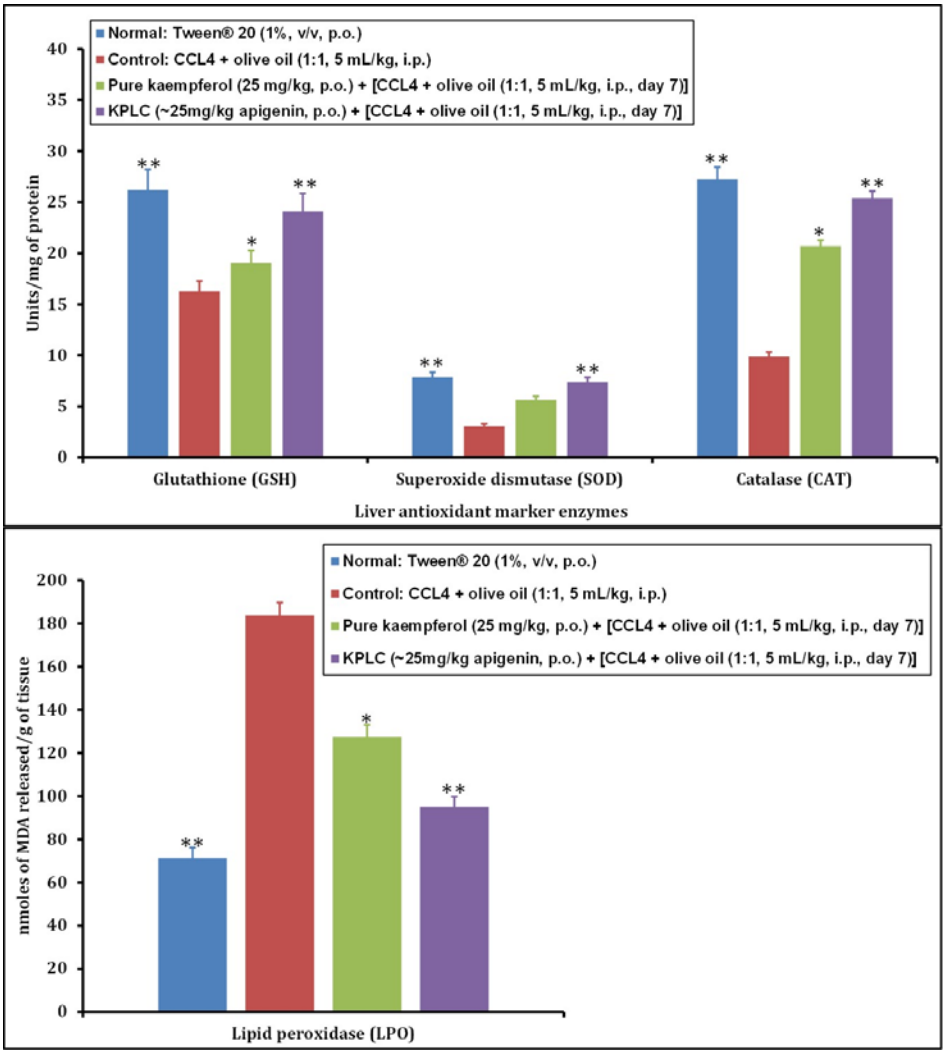

Figure 7 The *in vitro* dissolution profiles of kaempferol release from kaempferol suspension, and KPLC. Values are mean ± Std. Dev. (n = 3). *p < 0.05, **p < 0.01, ***p < 0.001 (significant with respect to pure kaempferol).

The observed increase in the kaempferol dissolution from KPLC may be attributed to its increased aqueous solubility in the complex. Moreover, increased wettability of the complex may also have contributed to the observed increase in the rate and extent of dissolution (50).

Various kinetic models *viz.*, zero order, first order, Higuchi, and Korsmeyer-Peppas model were explored to determine the model-fit of the release profile of KPLC (data not shown). Based on the obtained value of the regression coefficient (R^2=0.9783), the Higuchi model was found to be the best representative model describing the dissolution of KPLC. Additionally, the release exponent value (n) was estimated to be 0.47, thus indicating a non-Fickian release. The release mechanism of kaempferol, as determined by the Korsmeyer-Peppas model, was a two-step diffusion. The dissociation of kaempferol molecules from the KPLC matrix was followed by the diffusion of kaempferol molecules out the phospholipid matrix (51). Thus, KPLC was found to

significantly enhance both the rate and the extent of kaempferol release compared to pure kaempferol.

In Vivo antioxidant activity

Liver function test

Table 4 shows the results of influence of pure kaempferol and KPLC on the markers of CCl_4-induced hepatic damage in rats. CCl_4 is known to be bio-transformed by the liver CYP450 enzymes to produce free radicals. These free radicals covalently bind to cellular macromolecules (e.g. lipids, nucleic acids, proteins, etc.) and result in oxidative damage to several vital organs such as heart, kidney, brain, and liver (52). The rats treated with CCl_4 alone showed a significant increase in the marker enzymes viz., SGOT, SGPT, SALP, and total bilirubin. A significant ($p<0.05$) prevention of this increase was observed in rat treated with pure kaempferol (25 mg/kg, p.o.) for 7 consecutive days. Additionally, the rats treated with KPLC (~25mg/kg kaempferol, p.o.) for 7 consecutive days also showed a significantly ($p<0.01$) improved hepatoprotective activity by preventing the increase in the levels of these markers after CCl_4 administration.

In vivo antioxidant marker enzyme estimation

Several studies have reported the reliability of the levels of hepatic enzymes GSH, SOD, CAT, and LPO as indicators of *in vivo* antioxidant activity (17, 18, 29, 52, 53). Kaempferol is reported to have excellent antioxidant and hepatoprotective properties (2, 3). The results of the influence of pure kaempferol and KPLC on the levels of GSH, SOD, CAT, and LPO in CCl_4-treated and naïve mice are shown in Figure 8. Animals treated with CCl_4 alone showed a significant ($p<0.05$) reduction in the levels of GSH compared to animals receiving vehicle.

Table 4 Effect of pure kaempferol and KPLC on CCl_4-intoxicated rat hepatic marker enzymes, Serum Glutamic-Pyruvate Transaminase (SGPT), Serum Glutamic – Oxaloacetate Transaminase (SGOT), Alkaline Phosphatase (ALP), and total bilirubin.

ANIMAL TREATMENT GROUPS	SGPT (IU/L)[a]	SGOT (IU/L)[a]	SALP (IU/L)[a]	TOTAL BILIRUBIN (mg/dL)
(Group I) Normal Tween® 20 (1%, v/v, p.o.)	23.05 ± 1.58**	24.30 ±1.54**	142.60 ± 2.20**	0.37 ± 0.03**
(Group II) Control: CCl_4 + olive oil (1:1, 5 mL/kg, i.p.)	40.16 ±2.74	49.21 ± 2.91	179.30 ± 4.14	0.79 ± 0.05
(Group III) Kaempferol (25 mg/kg, p.o.) + [CCl_4 + olive oil (1:1, 5 mL/kg, i.p., day 7)]	33.28 ± 1.27*	42.10 ± 2.31*	166.15 ± 2.72*	0.55 ± 0.03*
(Group IV) KPLC (~25 mg/kg, p.o.) [CCl_4 + olive oil (1:1, 5 mL/kg, i.p., day 7)]	25.19 ± 1.11**	28.35 ± 2.12**	149.20 ± 2.05**	0.42 ± 0.02**

[a] - IU/L = International Units/Liter of Plasma,
All values are expressed as Mean ± Std. Error of Mean ($n = 6$)
*$p<0.05$, **$p<0.01$ (Significant with respect to control group)

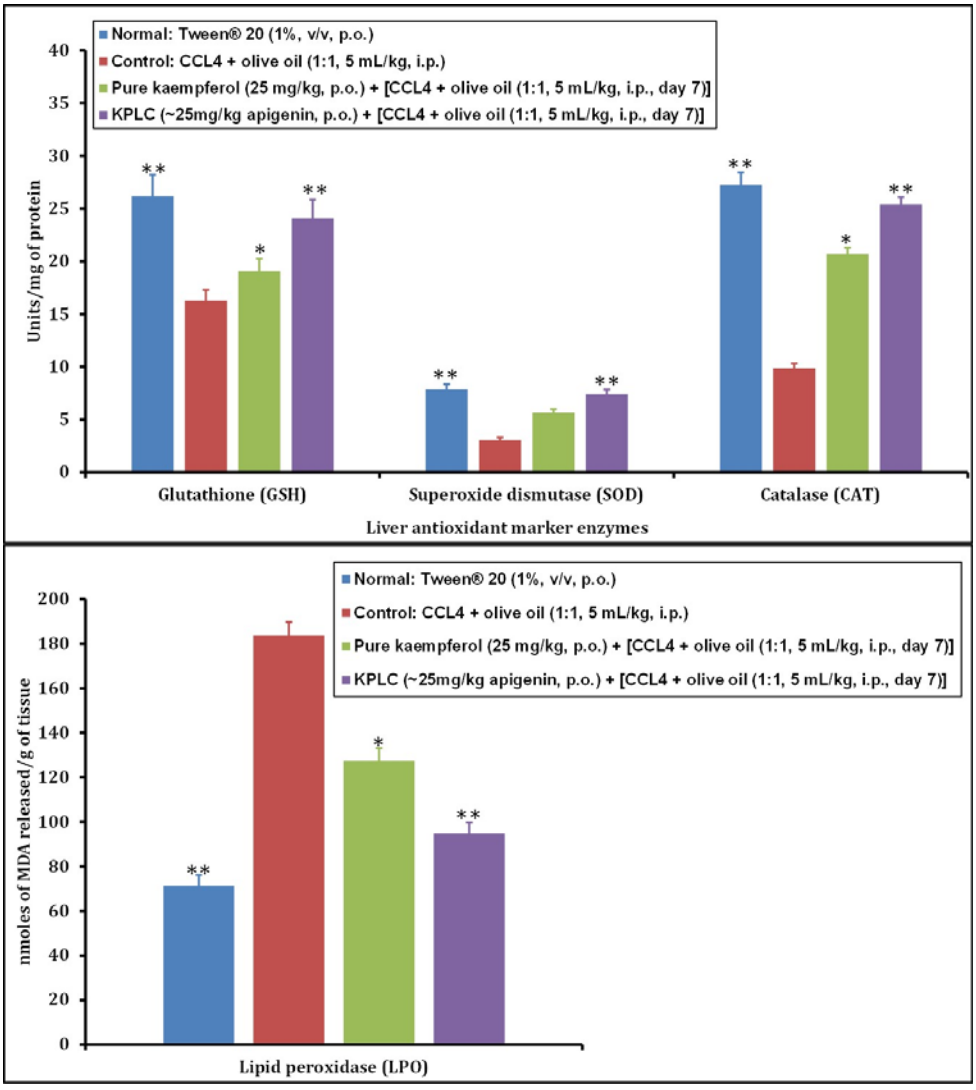

Figure 8 Influence of pure kaempferol and KPLC on rat liver antioxidant marker enzymes, i.e. glutathione reductase (GSH) (nmoles/mg of protein), superoxide dismutase (SOD) (units/mg protein), catalase (CAT) (units/mg protein), and lipid peroxidation (LPO) (nmoles of MDA released /g tissue). Values are Mean ± Std. Error of Mean (n = 6). *p < 0.05, **p < 0.01 (significant with respect to control: CCl_4-only treated groups).

The animal group receiving pure kaempferol exhibited a significant (p<0.05) prevention against CCl_4-induced reduction in GSH levels. The CCl_4-induced lowering of GSH levels in the liver homogenate was also prevented, albeit with a higher significance (p< 0.01) after treatment with KPLC (~25 mg/kg kaempferol, p.o.). The treatment with CCl_4 revealed a significant (p<0.01) reduction in the SOD levels in rat liver homogenate. The animal group treated with pure kaempferol (25 mg/kg, p.o.) resulted in a significant (p<0.05) prevention of CCl_4-induced reduction in SOD levels. Treatment with KPLC (~25 mg/kg kaempferol, p.o.) further prevented CCl_4-induced lowering of SOD significantly

(p<0.01). The levels of the enzyme CAT were observed to decrease significantly (p<0.01) after treatment with CCl_4, compared to animals receiving vehicle alone. Oral treatment with pure kaempferol (25 mg/kg, p.o.) significantly (p< 0.05) prevented this CCl_4-induced reduction in CAT levels. Kaempferol was found to be more effective, and highly significant (p<0.01) in preventing CCl_4-induced reduction in CAT levels when administered in the form of KPLC. Lipid peroxidation, measured as MDA (nM/g) in hemoglobin was found to increase significantly (p<0.01) after CCl_4 treatment. The administration of pure kaempferol (25 mg/kg, p.o.) prevented CCl_4-induced lipid peroxidation significantly (p<0.05). The animal group treated with KPLC (~25 mg/kg apigenin, p.o.) also showed a prevention of CCl_4-induced increase in lipid peroxidation, albeit with a higher significance (p< 0.01).

Histopathological studies

The influence of pure kaempferol, or KPLC treatment on the CCl_4-induced hepatic damage was assessed by investigating the histopathology of rat liver tissues. The hematoxylin-eosin stained microscopic (400×) images of liver tissues after treatment with Tween® 20, CCl_4, pure kaempferol + CCl_4, or KPLC+ CCl_4 are shown in the Figure 9A, 9B, 9C, and 9D, respectively. The animals treated with vehicle, i.e. Tween® 20 (1%, v/v) showed well-preserved hepatic cellular organelles indicating healthy, well-functioning liver physiology (Figure 9A). Treatment with CCl_4 appeared to result in a significant and a visible degeneration of parenchymal cells and fatty tissues, and a significant damage to the central lobular vein (Figure 9B). Pure kaempferol treatment (25 mg/kg, p.o.) exhibited a degree of hepatoprotective activity against CCl_4-induced hepatic damage (Figure 9C). The animals receiving KPLC (~25 mg/kg kaempferol, p.o.) demonstrated a significant protection against CCl_4-induced hepatic degeneration (Figure 9D). Thus, the antioxidant properties of kaempferol, both in pure form and in KPLC were evident by the restoration of normal anatomy of the hepatic cellular structures after these treatments.

Oral bioavailability studies

The oral bioavailability of pure kaempferol and KPLC was determined by analyzing the rat plasma samples via HPLC method. The peak resolution, signal-to-noise ratio, and the duration of sample analysis were improved by optimizing the chromatographic conditions. In this study, we used quercetin as internal standard, due to its structural similarity with pure kaempferol. In order to produce optimal sensitivity and peak resolution efficiency between kaempferol and quercetin, various solvent/buffer systems were evaluated. Acetonitrile was found to be an optimal mobile phase for resolving kaempferol and quercetin peaks, with an acceptable run time of 6.0 minutes. It was also observed that the addition of phosphoric acid (0.4%) to acetonitrile significantly improved the peak shape and resolution efficiency. The wavelength of 360 nm was chosen for the detection of both components.

In addition to the HPLC method optimization, it was important to identify an optimal technique for the extraction of kaempferol from plasma. Commonly employed techniques for drug extraction from plasma include solid-liquid extraction, liquid-liquid extraction, and protein precipitation. Solid-liquid extraction is known to exhibit excellent recovery and reproducibility. The technique, however, is reported to be complex and expensive, and limited to the rapid processing of multiple samples (54). Due to multiple extracting steps involved, the protein precipitation technique is cost-prohibitive, and the sample recovery also reported as being rather low (55, 56). Thus, for the current study, the plasma samples were processed using liquid-liquid extraction via

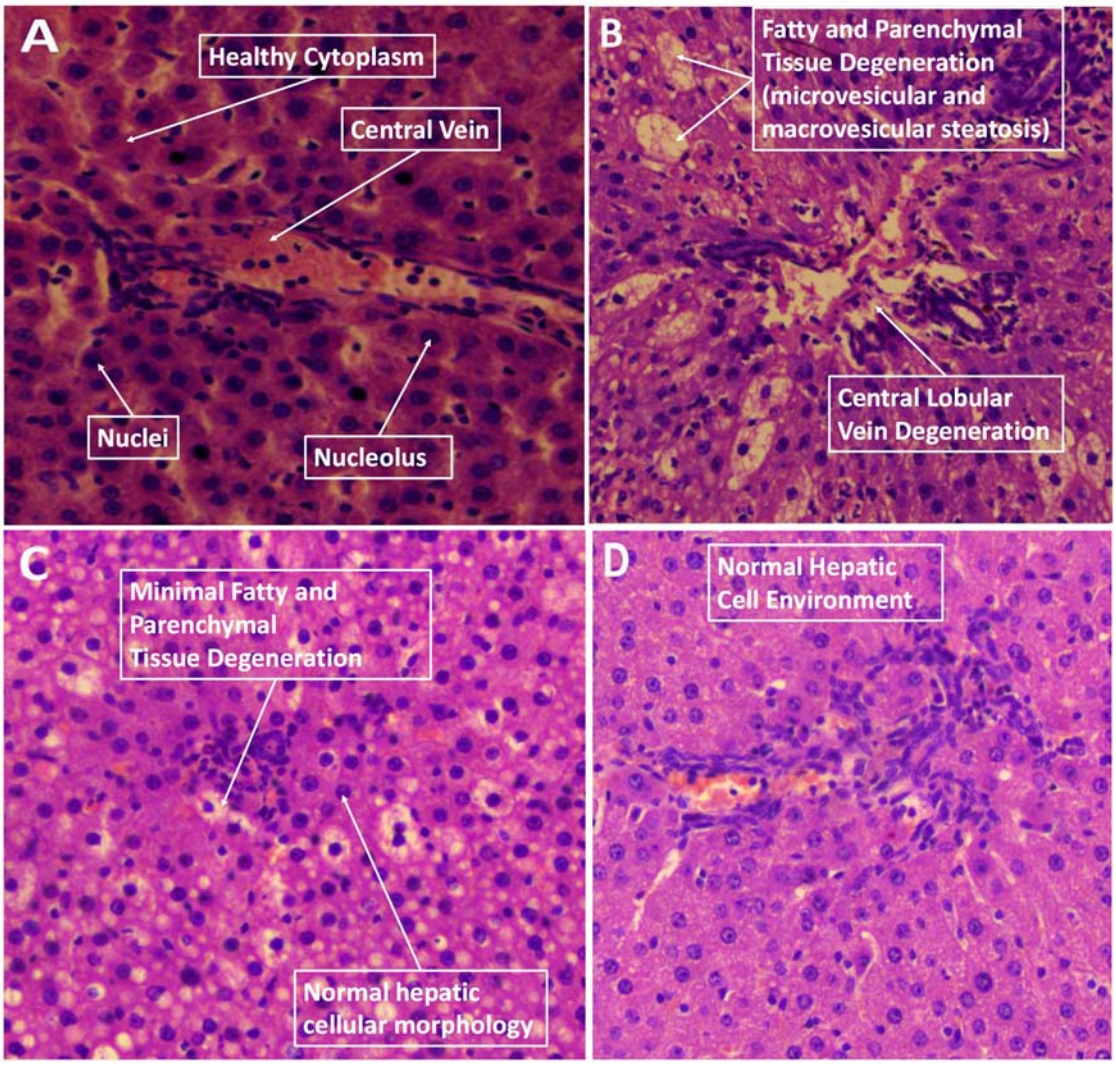

Figure 9 Histopathology micrographs (×400) of rat livers. (A) Normal: Tween® 20 (1%, v/v, p.o.), (B) Control: CCL_4 + olive oil (1:1, 5 mL/kg, i.p.), (C) Pure kaempferol (25 mg/kg, p.o.) + [CCL_4 + olive oil (1:1, 5 mL/kg, i.p., day 7)], and (D) KPLC (~25 mg/kg kaempferol, p.o.) + [CCL_4 + olive oil (1:1, 5 mL/kg, i.p., day 7)].

hydrolysis with hydrochloric acid (0.2 M). With this technique a high recovery was observed , as well as, accuracy in detecting kaempferol and quercetin.

Figure 10 shows the mean plasma concentration-time profiles of kaempferol in the plasma of animals treated with pure kaempferol (100 mg/kg, p.o.) or KPLC (~100 mg/kg, p.o.). The group treated with KPLC exhibited a significantly higher plasma concentration of kaempferol compared to the group treated with pure kaempferol, between 30 minutes and 8 hours. The concentration-time profile of pure kaempferol showed a near-plateau form with the levels of kaempferol never exceeding 0.2 µg/ml during the analysis period. The pharmacokinetic profile of KPLC exhibited an immediate increase in plasma kaempferol concentration, which peaked to ~1.5 µg/ml at 30 minutes. This was followed by a steady decrease in plasma kaempferol

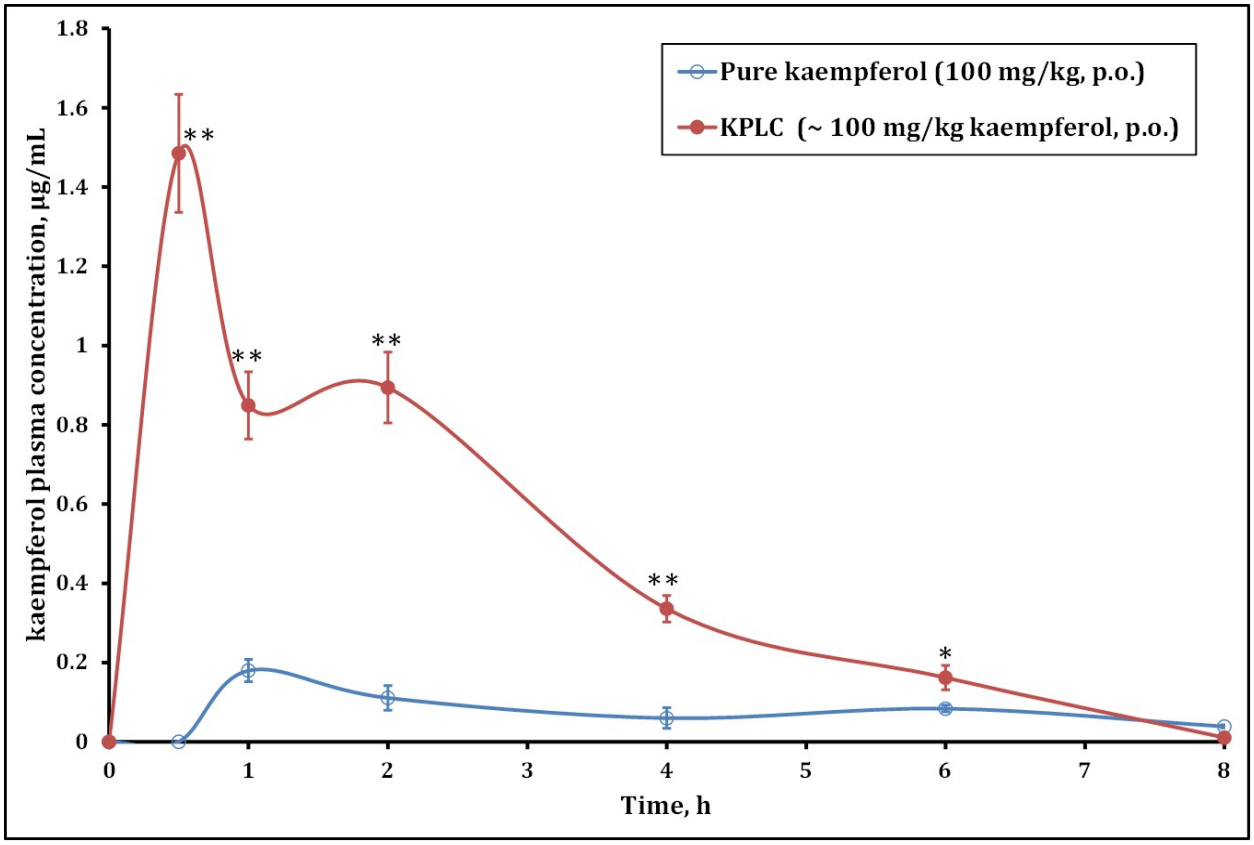

Figure 10 Mean plasma concentration-time profile after oral administration of pure kaempferol (100 mg/kg, p.o.) or KPLC (~100 mg/kg kaempferol, p.o.). Values are mean ± Std. Dev. (n = 6). *$p < 0.05$; **$p < 0.01$, and ***$p < 0.001$ (significant with respect to pure kaempferol treated group).

concentration for a period of 8 hours.

Table 5 lists the pharmacokinetic parameters calculated from the plasma concentration-time profiles, using a statistical software (WinNonlin®, Version 4.1, Certara USA Inc., Princeton, NJ, USA). The calculated values of bioavailability-indicating pharmacokinetic parameters such as C_{max}, T_{max}, and $AUC_{0-\infty}$ were found to be significantly higher in the treatment group receiving KPLC, compared to that receiving pure kaempferol. Additionally, this group also exhibited significantly lower values for elimination half-life ($t_{½\ el}$), clearance (cl/F), and volume of distribution (V_z/F). The elimination rate constant (K_{el}) however, was found to be higher in the group treated with KPLC compared to that treated with pure kaempferol. Additionally, the calculated bioavailability (F) of kaempferol after KPLC administration was observed to be ~100%. These observations led us to infer that KPLC treatment resulted in higher bioavailability and prolonged *in vivo* presence of kaempferol.

Complexation with phospholipid molecules, resulting in increased aqueous solubility and gastrointestinal absorption, is likely responsible for the enhanced relative bioavailability of kaempferol observed after a single oral administration of KPLC. While phospholipid-based complexation has exhibited enhanced bioavailability of kaempferol, factors such as dietary lipid intake and other internal or external factors may significantly affect the rate

Table 5 Pharmacokinetic parameters, for group of animals after oral administration of pure kaempferol (25 mg/kg, p.o.) and KPLC (~25 mg/kg, p.o.)

PHARMACOKINETIC PARAMETERS	TREATMENT	
	PURE KAEMPFEROL (100 mg/kg, p.o.)*	KPLC (~100 mg/kg of kaempferol, p.o.)*
C_{max} (µg ml^{-1})	0.18 ± 0.12	1.48 ± 0.41
T_{max} (hours)	1.0 ± 0.51	0.5 ± 0.37
Area under concentration –time curve (AUC_{0-t}) ((µg ml^{-1} h)	0.67 ± 0.21	3.72 ± 0.58
Area under concentration –time curve ($AUC_{0-\infty}$) ((µg ml^{-1} h)	0.89 ± 0.41	3.74 ± 0.73
Elimination half-life($t_{1/2el}$) (h)	3.85 ± 0.16	1.20 ± 0.24
Elimination rate constant (*Kel*) (h^{-1})	0.17 ± 0.04	0.57 ± 0.02
Clearance (*cl/F*) [(mg)/(µgml^{-1}h^{-1})]	112.32 ± 1.69	26.69 ± 0.83
Volume of distribution (*Vz/F*) [(mg)/(µgml^{-1}h^{-1})]	624.39 ± 0.57	46.47 ± 0.42

*Values are expressed as mean ± Std. Error of Mean (n = 6)

and extent of drug absorption from such systems. It is important to consider the use of suitable biorelevant media, and other experimental conditions when evaluating the solubility and permeability of drugs via such systems (57).

CONCLUSIONS

Improved aqueous solubility and oral bioavailability, resulting in excellent *in vivo* antioxidant activity of kaempferol with phospholipid-based complex, were the main outcomes of the present work. The study presented a simple, yet robust, method to prepare a KPLC formulation, optimized using a full-factorial design. Characterization by DSC, FTIR, ^{1}H-NMR, and PXRD supported the formation of a stable complex via non-covalent bonding interactions such as hydrogen bonding, ion-dipole, and van der Waals interactions. The increased aqueous solubility of the prepared KPLC as compared to PM or pure kaempferol was demonstrated by solubility analysis. Functional characterization revealed the enhanced dissolution of KPLC compared to pure kaempferol. The *in vivo* antioxidant activity of KPLC was also shown to be relatively higher compared to that of pure kaempferol, in a small rodent hepatotoxicity model. The analysis of pharmacokinetic parameters revealed an enhanced oral bioavailability of kaempferol from the prepared complex. The value of using phospholipids to improve the solubility, oral bioavailability and pharmacological properties, is further validated by this study.

ACKNOWLEDGEMENTS

The authors are thankful to the R.T.M. Nagpur University, Nagpur, Maharashtra, India, for the financial assistance to support this research project (DS/RTM/2013–14/2076).

REFERENCES

1 Kong L, Luo C, Li X, Zhou Y, He H. The anti-inflammatory effect of kaempferol on early atherosclerosis in high cholesterol fed rabbits. Lipids Health Dis. 2013;12:115. doi: 10.1186/1476-511x-12-115.

2 Vellosa JCR, Regasini LO, Khalil NM, Bolzani VdS, Khalil OAK, Manente FA, *et. al.*. Antioxidant and cytotoxic studies for kaempferol, quercetin and isoquercitrin. Eclética Química. 2011;36:07-20.

3 Park JS, Rho HS, Kim DH, Chang IS. Enzymatic preparation of kaempferol from green tea seed and its antioxidant activity. J Agric Food Chem.

2006;54(8):2951-6. doi:10.1021/jf052900a.

4 Youssef Moustafa AM, Khodair AI, Saleh MA. Isolation, structural elucidation of flavonoid constituents from Leptadenia pyrotechnica and evaluation of their toxicity and antitumor activity. Pharm Biol. 2009;47(6):539-52. doi: 10.1080/13880200902875065.

5 Rho HS, Ghimeray AK, Yoo DS, Ahn SM, Kwon SS, Lee KH, *et. al.*. Kaempferol and kaempferol rhamnosides with depigmenting and anti-inflammatory properties. Molecules. 2011;16(4):3338-44. doi: 10.3390/molecules16043338.

6 Li S, Pu X-P. Neuroprotective Effect of Kaempferol against a 1-Methyl-4-phenyl-1,2,3,6-tetrahydropyridine -Induced Mouse Model of Parkinson's Disease. Biol Pharm Bull. 2011;34(8):1291-6. doi: 10.1248/bpb.34.1291.

7 Guo AJ, Choi RC, Zheng KY, Chen VP, Dong TT, Wang Z-T, *et. al.*. Kaempferol as a flavonoid induces osteoblastic differentiation via estrogen receptor signaling. Chin Med. 2012;7(1):10. doi: 10.1186/1749-8546-7-10.

8 Barve A, Chen C, Hebbar V, Desiderio J, Saw CL, Kong AN. Metabolism, oral bioavailability and pharmacokinetics of chemopreventive kaempferol in rats. Biopharm Drug Dispos. 2009;30(7):356-65. doi: 10.1002/bdd.677.

9 Seguin J, Brulle L, Boyer R, Lu YM, Ramos Romano M, Touil YS, *et. al.*. Liposomal encapsulation of the natural flavonoid fisetin improves bioavailability and antitumor efficacy. Int J Pharm. 2013;444(1-2):146-54. doi: 10.1016/j.ijpharm.2013.01.050.

10 Ruan J, Liu J, Zhu D, Gong T, Yang F, Hao X, *et. al.*. Preparation and evaluation of self-nanoemulsified drug delivery systems (SNEDDSs) of matrine based on drug–phospholipid complex technique. Int J Pharm. 2010;386(1–2):282-90. doi: http://dx.doi.org/10.1016/j.ijpharm.2009.11.026.

11 Bhattacharyya S, Ahmmed SM, Saha BP, Mukherjee PK. Soya phospholipid complex of mangiferin enhances its hepatoprotectivity by improving its bioavailability and pharmacokinetics. J Sci Food Agric. 2014;94(7):1380-8. doi: 10.1002/jsfa.6422.

12 Zhang K, Gu L, Chen J, Zhang Y, Jiang Y, Zhao L, *et. al.*. Preparation and evaluation of kaempferol-phospholipid complex for pharmacokinetics and bioavailability in SD rats. J Pharm Biomed Anal. 2015;114:168-75. doi: 10.1016/j.jpba.2015.05.017.

13 Hou Z, Li Y, Huang Y, Zhou C, Lin J, Wang Y, *et. al.*. Phytosomes loaded with mitomycin C-soybean phosphatidylcholine complex developed for drug delivery. Mol Pharm. 2013;10(1):90-101. doi: 10.1021/mp300489p.

14 Tan Q, Liu S, Chen X, Wu M, Wang H, Yin H, *et. al.*. Design and evaluation of a novel evodiamine-phospholipid complex for improved oral bioavailability. AAPS PharmSciTech. 2012;13(2):534-47. doi: 10.1208/s12249-012-9772-9.

15 Saoji SD, Belgamwar VS, Dharashivkar SS, Rode AA, Mack C, Dave VS. The Study of the Influence of Formulation and Process Variables on the Functional Attributes of Simvastatin–Phospholipid Complex. J Pharm Innov. 2016:1-15. doi: 10.1007/s12247-016-9256-7.

16 Saoji SD, Dave VS, Dhore PW, Bobde YS, Mack C, Gupta D, *et. al.*. The role of phospholipid as a solubility- and permeability-enhancing excipient for the improved delivery of the bioactive phytoconstituents of Bacopa monnieri. Eur J Pharm Sci. 2016. doi: http://dx.doi.org/10.1016/j.ejps.2016.08.056.

17 Maiti K, Mukherjee K, Murugan V, Saha BP, Mukherjee PK. Exploring the Effect of Hesperetin–HSPC Complex—A Novel Drug Delivery System on the In Vitro Release, Therapeutic Efficacy and Pharmacokinetics. AAPS PharmSciTech. 2009;10(3):943. doi: 10.1208/s12249-009-9282-6.

18 Bhattacharyya S, Ahammed SM, Saha BP, Mukherjee PK. The gallic acid-phospholipid complex improved the antioxidant potential of gallic acid by enhancing its bioavailability. AAPS PharmSciTech. 2013;14(3):1025-33. doi: 10.1208/s12249-013-9991-8.

19 Reitman S, Frankel S. A colorimetric method for the determination of serum glutamic oxalacetic and glutamic pyruvic transaminases. Am J Clin Pathol. 1957;28(1):56-63.

20 Kind PRN, King EJ. Estimation of Plasma Phosphatase by Determination of Hydrolysed Phenol with Amino-antipyrine. J Clin Pathol. 1954;7(4):322-6.

21 Malloy HT, Evelyn KA. The Determination of Bilirubin with the Photoelectric Colorimeter. J Biol Chem. 1937;119(2):481-90.

22 Ellman GL. Tissue sulfhydryl groups. Arch Biochem Biophys. 1959;82(1):70-7. doi: http://dx.doi.org/10.1016/0003-9861(59)90090-6.

23 Marklund S, Marklund G. Involvement of the superoxide anion radical in the autoxidation of pyrogallol and a convenient assay for superoxide dismutase. Eur J Biochem. 1974;47(3):469-74.

24 Stocks J, Dormandy TL. The Autoxidation of Human Red Cell Lipids Induced by Hydrogen Peroxide. Br J Haematol. 1971;20(1):95-111. doi:

10.1111/j.1365-2141.1971.tb00790.x.

25 Beers RF, Jr., Sizer IW. A spectrophotometric method for measuring the breakdown of hydrogen peroxide by catalase. J Biol Chem. 1952;195(1):133-40.

26 Chen ZP, Sun J, Chen HX, Xiao YY, Liu D, Chen J, *et. al.*. Comparative pharmacokinetics and bioavailability studies of quercetin, kaempferol and isorhamnetin after oral administration of Ginkgo biloba extracts, Ginkgo biloba extract phospholipid complexes and Ginkgo biloba extract solid dispersions in rats. Fitoterapia. 2010;81(8):1045-52. doi: 10.1016/j.fitote.2010.06.028.

27 Jabbari M, Gharib F. Solvent dependence on antioxidant activity of some water-insoluble flavonoids and their cerium(IV) complexes. J Mol Liq. 2012;168:36-41. doi: http://dx.doi.org/10.1016/j.molliq.2012.02.001.

28 Bhattacharyya S, Majhi S, Saha BP, Mukherjee PK. Chlorogenic acid-phospholipid complex improve protection against UVA induced oxidative stress. J Photochem Photobiol B. 2014;130:293-8. doi: 10.1016/j.jphotobiol.2013.11.020.

29 Maiti K, Mukherjee K, Gantait A, Saha BP, Mukherjee PK. Curcumin–phospholipid complex: Preparation, therapeutic evaluation and pharmacokinetic study in rats. Int J Pharm. 2007;330(1–2):155-63. doi: http://dx.doi.org/10.1016/j.ijpharm.2006.09.025.

30 Qin X, Yang Y, Fan TT, Gong T, Zhang XN, Huang Y. Preparation, characterization and in vivo evaluation of bergenin-phospholipid complex. Acta Pharmacol Sin. 2010;31(1):127-36. doi: 10.1038/aps.2009.171.

31 Xia HJ, Zhang ZH, Jin X, Hu Q, Chen XY, Jia XB. A novel drug-phospholipid complex enriched with micelles: preparation and evaluation in vitro and in vivo. Int J Nanomedicine. 2013;8:545-54. doi: 10.2147/ijn.s39526.

32 Dhore PW, Dave VS, Saoji SD, Bobde YS, Mack C, Raut NA. Enhancement of the aqueous solubility and permeability of a poorly water soluble drug ritonavir via lyophilized milk-based solid dispersions. Pharm Dev Technol. 2016:1-13. doi: 10.1080/10837450.2016.1193193.

33 Freitas C, Müller RH. Effect of light and temperature on zeta potential and physical stability in solid lipid nanoparticle (SLN™) dispersions. Int J Pharm. 1998;168(2):221-9. doi: http://dx.doi.org/10.1016/S0378-5173(98)00092-1.

34 Freag MS, Elnaggar YS, Abdallah OY. Lyophilized phytosomal nanocarriers as platforms for enhanced diosmin delivery: optimization and ex vivo permeation. Int J Nanomedicine. 2013;8:2385-97. doi: 10.2147/ijn.s45231.

35 Li J, Liu P, Liu JP, Yang JK, Zhang WL, Fan YQ, *et. al.*. Bioavailability and foam cells permeability enhancement of Salvianolic acid B pellets based on drug-phospholipids complex technique. Eur J Pharm Biopharm. 2013;83(1):76-86. doi: 10.1016/j.ejpb.2012.09.021.

36 Singh C, Bhatt TD, Gill MS, Suresh S. Novel rifampicin–phospholipid complex for tubercular therapy: Synthesis, physicochemical characterization and in-vivo evaluation. Int J Pharm. 2014;460(1–2):220-7. doi: http://dx.doi.org/10.1016/j.ijpharm.2013.10.043.

37 Yanyu X, Yunmei S, Zhipeng C, Qineng P. The preparation of silybin–phospholipid complex and the study on its pharmacokinetics in rats. Int J Pharm. 2006;307(1):77-82. doi: http://dx.doi.org/10.1016/j.ijpharm.2005.10.001.

38 Galasso V, Asaro F, Berti F, Pergolese B, Kovač B, Pichierri F. On the molecular and electronic structure of matrine-type alkaloids. Chem Phys. 2006;330(3):457-68. doi: http://dx.doi.org/10.1016/j.chemphys.2006.09.017.

39 Lasonder E, Weringa WD. An NMR and DSC study of the interaction of phospholipid vesicles with some anti-inflammatory agents. J Colloid Interface Sci. 1990;139(2):469-78. doi: http://dx.doi.org/10.1016/0021-9797(90)90119-9.

40 Venema FR, Weringa WD. The interactions of phospholipid vesicles with some anti-inflammatory agents. J Colloid Interface Sci. 1988;125(2):484-92. doi: http://dx.doi.org/10.1016/0021-9797(88)90013-6.

41 Sharma P, Sarin R. Isolation and Characterization of Quercetin and Kaempferol in vivo and in vitro from Pedalium murex. Int Res J Pharm. 2012;3(6):184-7.

42 Semalty A, Semalty M, Singh D, Rawat MSM. Phyto-phospholipid complex of catechin in value added herbal drug delivery. J Inclusion Phenom Macrocyclic Chem. 2012;73(1):377-86. doi: 10.1007/s10847-011-0074-8.

43 Singh D, Rawat MSM, Semalty A, Semalty M. Chrysophanol–phospholipid complex. J Therm Anal Calorim. 2012;111(3):2069-77. doi: 10.1007/s10973-012-2448-6.

44 Zhang J, Tang Q, Xu X, Li N. Development and evaluation of a novel phytosome-loaded chitosan microsphere system for curcumin delivery. Int J Pharm. 2013;448(1):168-74. doi: http://dx.doi.org/10.1016/j.ijpharm.2013.03.021.

45 Semalty A, Semalty M, Singh D, Rawat MSM.

Preparation and characterization of phospholipid complexes of naringenin for effective drug delivery. J Inclusion Phenom Macrocyclic Chem. 2010;67(3):253-60. doi: 10.1007/s10847-009-9705-8.

46 Wang H, Cui Y, Fu Q, Deng B, Li G, Yang J, *et. al.*. A phospholipid complex to improve the oral bioavailability of flavonoids. Drug Dev Ind Pharm. 2015;41(10):1693-703. doi: 10.3109/03639045.2014.991402.

47 Cai X, Luan Y, Jiang Y, Song A, Shao W, Li Z, *et. al.*. Huperzine A-phospholipid complex-loaded biodegradable thermosensitive polymer gel for controlled drug release. Int J Pharm. 2012;433(1-2):102-11. doi: 10.1016/j.ijpharm.2012.05.009.

48 Yue P-F, Zhang W-J, Yuan H-L, Yang M, Zhu W-F, Cai P-L, *et. al.*. Process Optimization, Characterization and Pharmacokinetic Evaluation in Rats of Ursodeoxycholic Acid–Phospholipid Complex. AAPS PharmSciTech. 2008;9(1):322-9. doi: 10.1208/s12249-008-9040-1.

49 Yue PF, Zhang WJ, Yuan HL, Yang M, Zhu WF, Cai PL, *et. al.*. Process optimization, characterization and pharmacokinetic evaluation in rats of ursodeoxycholic acid-phospholipid complex. AAPS PharmSciTech. 2008;9(1):322-9. doi: 10.1208/s12249-008-9040-1.

50 Perrut M, Jung J, Leboeuf F. Enhancement of dissolution rate of poorly-soluble active ingredients by supercritical fluid processes: Part I: Micronization of neat particles. Int J Pharm. 2005;288(1):3-10. doi: http://dx.doi.org/10.1016/j.ijpharm.2004.09.007.

51 Dash S, Murthy PN, Nath L, Chowdhury P. Kinetic modeling on drug release from controlled drug delivery systems. Acta Pol Pharm. 2010;67(3):217-23.

52 Khan RA, Khan MR, Sahreen S, Shah NA. Hepatoprotective activity of Sonchus asper against carbon tetrachloride-induced injuries in male rats: a randomized controlled trial. BMC Complement Altern Med. 2012;12:90. doi: 10.1186/1472-6882-12-90.

53 Recknagel RO, Glende EA, Dolak JA, Waller RL. Mechanisms of carbon tetrachloride toxicity. Pharmacol Ther. 1989;43(1):139-54. doi: http://dx.doi.org/10.1016/0163-7258(89)90050-8.

54 Yang J, Lv F, Chen X-q, Cui W-x, Chen L-h, Wen X-d, *et. al.* Pharmacokinetic study of major bioactive components in rats after oral administration of extract of Ilex hainanensis by high-performance liquid chromatography/electrospray ionization mass spectrometry. J Pharm Biomed Anal. 2013;77:21-8. doi: http://dx.doi.org/10.1016/j.jpba.2013.01.011.

55 DuPont MS, Day AJ, Bennett RN, Mellon FA, Kroon PA. Absorption of kaempferol from endive, a source of kaempferol-3-glucuronide, in humans. Eur J Clin Nutr. 2004;58(6):947-54. doi: 10.1038/sj.ejcn.1601916.

56 Fong SY, Martins SM, Brandl M, Bauer-Brandl A. Solid Phospholipid Dispersions for Oral Delivery of Poorly Soluble Drugs: Investigation Into Celecoxib Incorporation and Solubility-In Vitro Permeability Enhancement. J Pharm Sci. 2016;105(3):1113-23. doi: 10.1016/s0022-3549(15)00186-0.